(Fig. 6C) in patients who had a partial response (PR) to cetuximab-based therapy (n = 16) than in those who had either stable disease (SD) or progressive disease (PD; n = 49). The same was true (P < 0.0001, t test) when the comparison was made only in patients with *KRAS* wild-type cancers (Fig. 6C). Because plasma heregulin may not fully reflect tumor heregulin concentrations, we asked whether tumor heregulin expression correlated with cetuximab efficacy. We isolated RNA from pretreatment tumor specimens in a subset of 44 of 70 (63%) patients, in whom tumor tissue was available, performed qPCR for heregulin (Fig. 6D), and correlated the findings with cetuximab efficacy. As in the ELISA studies, patients achieving a PR (n = 9) had significantly (P < 0.0001, t test) lower tumor heregulin expression compared to those with SD or PD (n = 35), whether we considered all patients or just those with *KRAS* wild-type (P = 0.0001, t test) cancers (Fig. 6D). We further divided the patients into two groups (low heregulin and high heregulin) based on the median plasma value (1622.5 pg/ml) and evaluated the relationship to PFS and OS. The low-heregulin group had significantly longer PFS (P = 0.004, log-rank test) and OS (P = 0.0014,

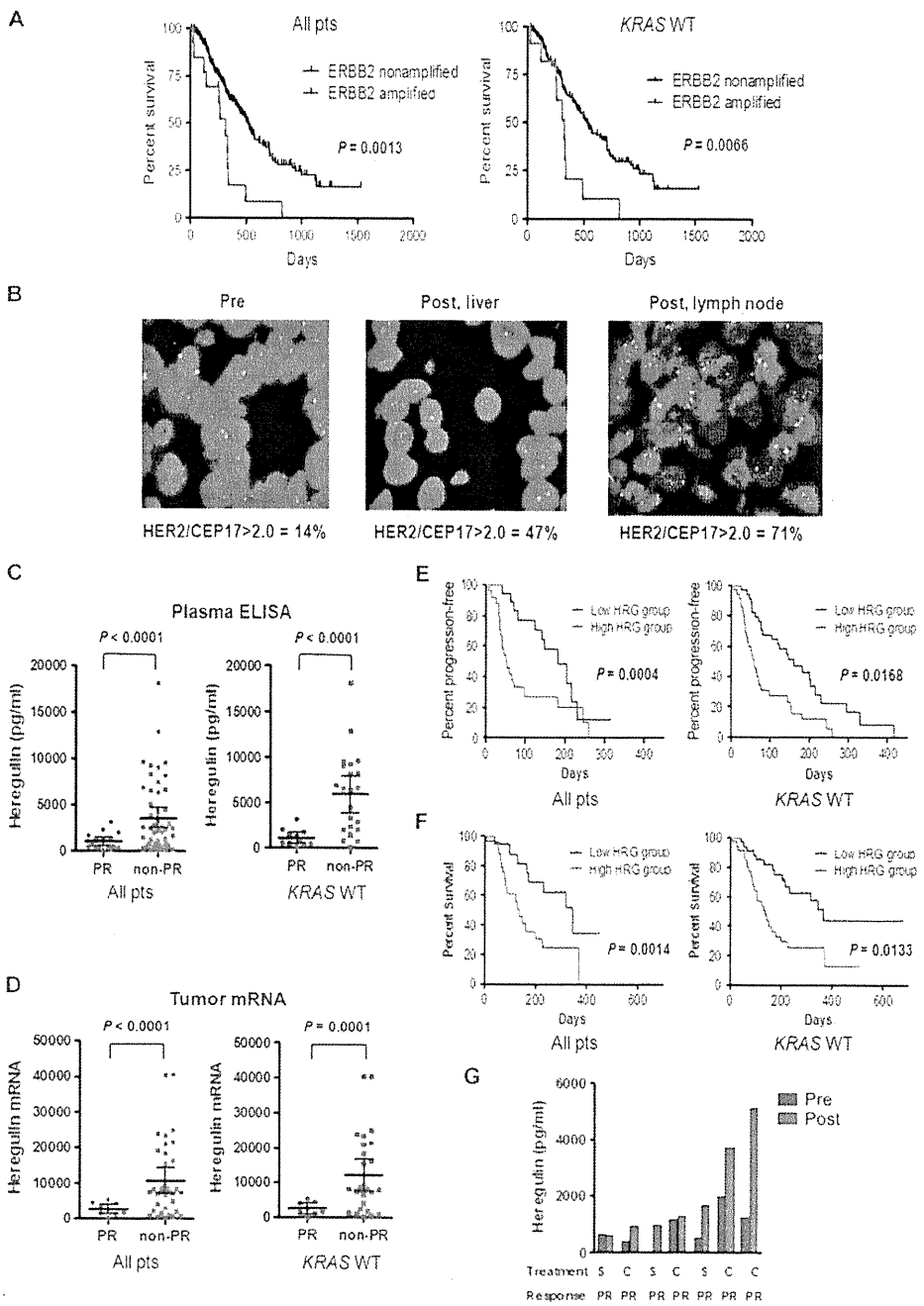

Fig. 6. Both *ERBB2* amplification and heregulin cause drug resistance in cetuximab-treated CRC patients. **(A)** (Left) OS for all CRC patients with (n = 13) and without (n = 220) *ERBB2* amplification treated with cetuximab-based therapy. Data for *KRAS* wild type (WT)–only patients (*ERBB2*-amplified, n = 11; *ERBB2* nonamplified, n = 171). Comparison based on log-rank test. **(B)** *ERBB2* FISH from a baseline primary tumor specimen (left) and after acquired cetuximab resistance in two independent drug-resistant specimens (right). The patient was initially treated with single-agent cetuximab and achieved a PR. ERBB2 (red) and CEP17 (green). **(C)** Scatter diagram of pretreatment heregulin concentration in plasma from all (n = 65) or *KRAS* wild type–only (n = 33) CRC patients achieving a PR and those not achieving a PR when treated with cetuximab-based therapy. Mean ± 95% CI is shown. **(D)** Scatter diagram of pretreatment heregulin mRNA expression in tumors from all (n = 44) or *KRAS* wild type–only (n = 34) CRC patients achieving a PR and those not achieving a PR when treated with cetuximab-based therapy. Mean ± 95% CI is shown. **(E)** (Left) PFS for all CRC patients treated with cetuximab-based therapy divided on the basis of low (n = 35) or high (n = 35) plasma expression. (Right) Data for *KRAS* wild type–only patients (low, n = 18; high, n = 24). Comparison based on log-rank test. **(F)** (Left) OS for all CRC patients treated with cetuximab-based therapy divided on the basis of low (n = 35) or high (n = 35) plasma expression. (Right) Data for *KRAS* wild type–only patients (low, n = 18; high, n = 24). Comparison based on log-rank test. **(G)** Comparisons of plasma levels of heregulin from CRC patients treated with cetuximab-based therapy before therapy and after the development of drug resistance. All patients achieved a PR. S, single-agent cetuximab; C, combination with irinotecan.

Downloaded from stm.sciencemag.org on February 25, 2012

log-rank test) compared to the high-heregulin group [median PFS, 161 versus 59 days; hazard ratio (HR), 0.36; 95% confidence interval (CI), 0.20 to 0.63; median OS, 366 versus 137 days; HR, 0.34; 95% CI, 0.18 to 0.66] when treated with cetuximab-based therapy (Fig. 6, E and F). This result was similar in *KRAS* wild-type patients (median PFS, 182 versus 52 days; HR, 0.41; 95% CI, 0.20 to 0.85; median OS, 345 versus 137 days; HR, 0.36; 95% CI, 0.16 to 0.80).

To evaluate the role of heregulin in acquired cetuximab resistance, we examined changes in serum heregulin levels after the development of drug resistance in seven patients, all of whom initially achieved a PR to cetuximab-based therapy (Fig. 6G). Compared to the pretreatment values, the posttreatment heregulin plasma concentrations were significantly higher ($P = 0.0313$, Wilcoxon signed-rank test) after the development of clinical cetuximab resistance (Fig. 6G). Collectively, these clinical studies further support our in vitro and in vivo studies and demonstrate that both *ERBB2* amplification and increased heregulin levels are associated with both de novo and acquired resistance to cetuximab-based therapy in CRC patients.

DISCUSSION

Studies of drug resistance mechanisms are critical for the development of effective cancer therapies. Mechanistic insights gained from studies of preclinical models and patient tumor specimens can be used to design new treatments or combination treatment strategies. This approach has led to the development of ABL kinase inhibitors for patients with imatinib-resistant chronic myeloid leukemia and the combination of EGFR and MET inhibitors for drug-resistant NSCLC (*12*, *25*, *26*).

Studies of drug resistance to EGFR inhibitors have focused on understanding resistance mechanisms to EGFR kinase inhibitors, and findings from the studies have been applied to develop the next generation of clinical trials (*12*, *27*, *28*). In contrast, there has been limited exploration of mechanisms of acquired resistance to EGFR-directed antibodies and none have been evaluated in cancer patients (*29*, *30*). Here, using a combination of resistant clones of cetuximab-sensitive cell lines coupled with analyses of cetuximab-treated CRC patients, we uncover aberrant ERBB2 signaling as a mediator of cetuximab resistance. We further demonstrate that aberrant ERBB2 signaling contributes to both de novo and acquired drug resistance in cetuximab-treated CRC patients.

Aberrant ERBB2 signaling (by *ERBB2* amplification or heregulin production) is an example of a resistance mechanism that leads to activation of a bypass signaling pathway. This is possible because ERBB2 is not the direct or indirect target of cetuximab. Both mechanisms of aberrant ERBB2 activation lead to persistent ERK1/2 signaling in the presence of cetuximab, thus preventing cetuximab-mediated growth inhibition (which is normally mediated by down-regulation of ERK1/2 signaling). In support of this hypothesis, both GEO and the *ERBB2*-amplified cetuximab-resistant GEO CR3 cells remain equally sensitive to the MEK inhibitor AZD6244. Notably, activation of EGFR signaling induces resistance to the ERBB2-directed therapeutic antibody trastuzumab in breast cancer cell lines in vitro and in vivo, suggesting a common mechanism for drug resistance to therapeutic antibodies in ERBB-driven cancers (*31*). *ERRB2* amplification is a unique mechanism of drug resistance in the case of cetuximab because *ERBB2*-amplified, cetuximab-resistant NSCLC cells remain sensitive to the EGFR kinase inhibitor gefitinib in vitro and in vivo (Fig. 5A and fig. S1A), likely because gefitinib, but not cetuximab, in addition to inhibiting EGFR, is also able to inhibit ERBB2 at clinically achievable concentrations (*32*).

Our findings are directly relevant to patients who develop acquired resistance to cetuximab-based therapy and may help guide subsequent treatment. Several agents that target ERBB2 signaling, including lapatinib and trastuzumab, are already approved and others, including irreversible ERBB2 kinase inhibitors and pertuzumab, are undergoing clinical development. Hence, the findings from the current study can be immediately used to design potential clinical therapies for CRC patients. Given the retrospective nature of the studies, these findings will need further clinical validation. The frequency and the relationship of *ERBB2* amplification to heregulin overexpression in cetuximab-resistant cancers need to be fully assessed in prospective studies. Our preclinical studies suggest that these are two independent means by which cancers can develop cetuximab resistance. However, whether *ERBB2* amplification and heregulin overexpression can occur together in the same drug-resistant tumor or tumor cells remains to be defined. It is intriguing that both increased levels of hepatocyte growth factor (HGF) and *MET* amplification have been observed in some EGFR kinase inhibitor–resistant NSCLCs (*16*).

Prospective clinical trials of cetuximab need to include evaluation of drug resistance mechanisms, including *ERBB2* amplification and heregulin measurements, at the time of disease progression. For patients with evidence of one of these drug resistance mechanisms, cetuximab combined with ERBB2-targeted therapy (for both mechanisms) or with an anti-ERBB3 antibody (heregulin only) should be further evaluated in clinical trials.

MATERIALS AND METHODS

Cell culture and reagents

The HCC827, H1648, HN11, GEO, A431, and DiFi cell lines have been previously characterized (*14*, *17*, *33*, *34*). Cetuximab and trastuzumab were purchased from the Dana-Farber Cancer Institute pharmacy. Gefitinib and lapatinib were purchased from American Custom Chemicals Corporation. Pertuzumab was provided by Roche Diagnostics. Cell proliferation and growth assays were performed with the MTS [3-(4,5-dimethylthiazol-2-yl)-5-(3-carboxymethoxyphenyl)-2-(4-sulfophenyl)-2*H*-tetrazolium, inner salt] assay as described (*12*). All experimental points were a result of 6 to 12 replicates, and all experiments were repeated at least three times. The data were graphically displayed with GraphPad Prism version 5.0 for Windows (GraphPad Software).

Generation of drug-resistant cell lines

To generate drug-resistant cell lines, we exposed HCC827, GEO, and A431 cells to increasing concentrations of cetuximab similar to previously described methods (*12*, *13*). Individual clones from cetuximab-resistant cells were isolated and confirmed to be resistant.

Antibodies and Western blotting

Cells grown under the previously specified conditions were lysed in NP-40 buffer. Western blot analyses were conducted after separation by SDS–polyacrylamide gel electrophoresis and transfer to nitrocellulose membranes. Immunoblotting was performed according to the antibody manufacturers' recommendations. Anti-pAKT (Ser^{473}), anti–total AKT, anti-pERBB2, anti-pERBB3, anti-ERBB2, and anti-EGFR antibodies

Downloaded from stm.sciencemag.org on February 25, 2012

were obtained from Cell Signaling Technology. The anti-heregulin antibody was purchased from NeoMarkers. The pEGFR (pY^{1068}), total ERK1/2, and pERK1/2 (pT^{185}/pY^{187}) antibodies were purchased from Invitrogen. Total ERBB3 antibody was purchased from Santa Cruz Biotechnology. The biotin-conjugated anti-EGFR antibody (ab24293) was obtained from Abcam. Relative pERK1/2 quantification was performed with the ImageJ 1.44 software.

Single-nucleotide polymorphism analyses

Single-nucleotide polymorphism (SNP) analyses were performed as described (*12*). Samples were processed for the Human Mapping 250K Sty SNP array according to the manufacturer's instructions. Comparison of gene copy number differences was performed with the dChip software according to previously established methods (*12*, *35*).

Site-directed mutagenesis

The *ERBB2* K753M (kinase dead) and the *BRAF* V600E mutations were introduced into *ERBB2* or *BRAF*, respectively, using site-directed mutagenesis with the QuikChange Site-Directed Mutagenesis kit according to the manufacturer's instructions (*14*). All constructs were confirmed by DNA sequencing. The constructs were shuttled into the retroviral vector JP1540 with the BD CreatorPP System (BD Biosciences). Retroviral infections were carried out as described (*36*). Cells infected with a GFP expression vector were used as a control.

FISH analyses

Cell suspensions were dropped onto precleaned slides and air-dried. Three-day-old slides were analyzed with the dual-color FISH assay with the PathVysion DNA probe set. The slides were incubated in 70% acetic acid for 40 s, digested in 0.008% pepsin/0.01 M HCl at 37°C for 5 min, fixed in 1% formaldehyde for 10 min, and dehydrated in an ethanol series. Formalin-fixed, paraffin-embedded (FFPE) tissue sections from CRC patients were subjected to a dual-color FISH assay with the PathVysion probe (LSI HER2 SO/CEP17 SG, Abbott Molecular). Initially, the slides were incubated from 2 hours to overnight at 56°C, deparaffinized in Citri-Solv, and washed in 100% ethanol for 10 min. The slides were sequentially incubated in 2× SSC at 75°C for 10 to 24 min, digested in proteinase K (0.25 mg/ml)/2× SSC at 45°C for 10 to 24 min, washed in 2× SSC for 5 min, and dehydrated in ethanol. The probe was applied according to the manufacturer's instructions to the selected hybridization area, which was covered with a glass coverslip and sealed with rubber cement. DNA denaturation was performed for 15 min at 85°C, and hybridization was allowed to occur at 37°C for 12 to 24 hours. Posthybridization washes were performed sequentially with 2× SSC/0.3% NP-40 (pH 7.0 to 7.5) at 73°C for 2 min and 2× SSC for 2 min, and dehydrated in ethanol. Chromatin was counterstained with 4′,6-diamidino-2-phenylindole (DAPI) (0.3 μg/ml) in Vectashield mounting medium (Vector Laboratories). Analysis was performed on an epifluorescence microscope with single interference filter sets for green [fluorescein isothiocyanate (FITC)], red (Texas red), blue (DAPI), dual (red/green), and triple (blue, red, green) band-pass filters.

shRNA and siRNA constructs and lentiviral infection

ERBB2 shRNA constructs cloned in pLKO.1 puro vector were described (*13*, *20*). A vector containing a nontargeting shRNA was used as a control. Lentivirus production, titrations, and infections were performed as in (*13*, *37*). The specific shRNA sequences are available upon request. The HRG1 (heregulin) siRNA was from Dharmacon (ON-TARGETplus SMARTpool #L-004608-01). HRG1 siRNA was a mixture of four sets of 21-nucleotide sense and antisense strands. ERBB2 siRNA was designed as follows: antisense, 5′-UGAGCUACCUGGAGGAUGUdTdT-3′. Control siRNA was nontargeting siRNA #1 (Dharmacon) and was used as a nonspecific control. For transfections, cells were plated at 50% confluence in six-well plates and incubated for 24 hours in RPMI 1640 supplemented with 0.1% fetal bovine serum (FBS). Cells were then treated with siRNAs mixed with Lipofectamine RNAiMax (Invitrogen).

Phospho-RTK array

Cells were lysed with NP-40 lysis buffer after incubation in RPMI 1640 supplemented with 0.1% FBS for 24 hours. Cell lysates were centrifuged at 14,000*g* for 5 min. Supernatants were transferred to and incubated with the Human Phospho-RTK Array (R&D Systems) according to the manufacturer's procedure.

Xenograft studies

The xenograft studies were performed with the HCC827 GFP, HCC827 ERBB2, A431, and A431 cetuximab-resistant cells as described (*38*). Cetuximab or pertuzumab was administered by intraperitoneal injection (cetuximab: 40 mg/kg, twice weekly; pertuzumab: 12 mg/kg, week 1 followed by 6 mg/kg weekly), and gefitinib (150 mg/kg per day) by oral gavage (*38*). The studies were performed in accordance with the standards of the Institutional Animal Care and Use Committee under a protocol approved by the Animal Care and Use Committee of the Beth Israel Deaconess Medical Center and the Kinki University.

Patients

Plasma and tumor specimens from CRC patients treated with cetuximab-based therapy were obtained from Istituto Clinico Humanitas (Rozzano, Italy), University Hospital of Heraklion (Heraklion, Greece), the Dana-Farber Cancer Institute/Brigham and Women's Hospital (Boston, MA), Kinki University Hospital (Osaka, Japan), Osaka City General Hospital (Osaka, Japan), Kinki University Sakai Hospital (Osaka, Japan), and the Kinki University Nara Hospital (Nara, Japan) under Institutional Review Board–approved studies. All patients provided written informed consent.

HER2 ECD measurements

Plasma specimens were obtained from nine CRC patients before cetuximab treatment and after development of acquired resistance to cetuximab. ERBB2/HER2 ECD was measured with an ELISA assay according to the manufacturer's recommended conditions (Siemens Healthcare Diagnostics). Only patients who developed PR or SD were included in these analyses. The studies were approved by the Institutional Review Board at the Kinki University.

KRAS sequencing

DNA was extracted from each tissue specimen with standard techniques. Codons 12 and 13 of exon 2 of *KRAS* were sequenced directly.

Quantitative heregulin PCR from cells and primary tumors

Total RNA was isolated from A431 and A431CR cells with the RNeasy Mini Kit (Qiagen), according to the manufacturer's specifications. The complementary DNA (cDNA) was synthesized with RT Enzyme Mix (Applied Biosystems) according to the manufacturer's specifications and was used for real-time PCR with SYBR Green (Cambrex Bio Science) to measure GAPDH (glyceraldehyde-3-phosphate dehydrogenase) and heregulin.

Downloaded from stm.sciencemag.org on February 25, 2012

All tumor specimen samples were formalin-fixed and paraffin-embedded. Tumor RNA was isolated from FFPE tumors with the RNeasy FFPE kit (Qiagen). RNA was extracted form DNA digestion with DNaseI according to the manufacturer's protocol. Reverse transcription was performed with a High Capacity RNA-to-cDNA Kit (Applied Biosystems) and was followed by quantitative reverse transcription–PCR (RT-PCR) with a Solaris qPCR GENE Expression Assays SYBR (Thermo Fischer Scientific) measured by ABI PRISM 7900HT (Applied Biosystems). Heregulin expression was measured in duplicate and normalized against the reference gene *GAPDH*.

Heregulin ELISA assay

Heregulin was measured in cell culture medium or human plasma with a sandwich ELISA (NRG1-β1 DuoSet) with methods as described (*17*). Cells were seeded in six-well plates at a concentration of 0.5×10^6 cells per well with RPMI 1640 supplemented with 10% FBS. After confluent growth, the medium was replaced with 5 ml of RPMI 1640 supplemented with 0.1% FBS. After a 48-hour incubation, cell culture medium was collected. Human plasma samples were obtained from CRC patients within a week before cetuximab treatment. All subjects provided written informed consent. In the case of patients who acquired resistance to cetuximab, samples were also obtained at the point of disease progression. After centrifugation at 15,000 rpm for 3 min, the supernatant was collected.

Statistical analysis

Statistical analysis was performed with the StatView statistical program (SAS Institute) to compare patient characteristics with responses to therapy. PFS and OS curves were generated with the Kaplan-Meier method, and differences based on *ERBB2* amplification and median heregulin plasma levels were evaluated with the log-rank test. All *P* values are two-sided.

SUPPLEMENTARY MATERIAL

www.sciencetranslationalmedicine.org/cgi/content/full/3/99/99ra86/DC1

Oligonucleotide sequences

Fig. S1. Cetuximab-resistant HCC827 and GEO cells.

Fig. S2. ERBB2 causes resistance to cetuximab in cetuximab-sensitive cells.

Fig. S3. ERBB2 maintains ERK1/2 signaling in the presence of cetuximab.

Fig. S4. Lapatinib restores sensitivity to cetuximab.

Fig. S5. Heregulin mediates resistance to cetuximab in A431 cells.

Fig. S6. Heregulin mediates resistance to cetuximab in the GEO cells.

Fig. S7. Progression-free survival for all CRC patients treated with cetuximab-based therapy.

Fig. S8. Increased *ERBB2* copy number is associated with acquired cetuximab resistance.

Table S1. Characteristics of colorectal cancer patients used to evaluate impact of *ERBB2* amplification.

Table S2. Clinical and treatment information on colorectal cancer patients used for plasma ERBB2 extracellular domain measurements.

Table S3. Characteristics of colorectal cancer patients used for plasma- and tumor-based studies of heregulin.

REFERENCES AND NOTES

1. D. J. Jonker, C. J. O'Callaghan, C. S. Karapetis, J. R. Zalcberg, D. Tu, H. J. Au, S. R. Berry, M. Krahn, T. Price, R. J. Simes, N. C. Tebbutt, G. van Hazel, R. Wierzbicki, C. Langer, M. J. Moore, Cetuximab for the treatment of colorectal cancer. *N. Engl. J. Med.* **357**, 2040–2048 (2007).
2. J. B. Vermorken, R. Mesia, F. Rivera, E. Remenar, A. Kawecki, S. Rottey, J. Erfan, D. Zabolotnyy, H. R. Kienzer, D. Cupissol, F. Peyrade, M. Benasso, I. Vynnychenko, D. De Raucourt, C. Bokemeyer, A. Schueler, N. Amellal, R. Hitt, Platinum-based chemotherapy plus cetuximab in head and neck cancer. *N. Engl. J. Med.* **359**, 1116–1127 (2008).
3. R. Pirker, J. R. Pereira, A. Szczesna, J. von Pawel, M. Krzakowski, R. Ramlau, I. Vynnychenko, K. Park, C. T. Yu, V. Ganul, J. K. Roh, E. Bajetta, K. O'Byrne, F. de Marinis, W. Eberhardt, T. Goddemeier, M. Emig, U. Gatzemeier; FLEX Study Team, Cetuximab plus chemotherapy in patients with advanced non-small-cell lung cancer (FLEX): An open-label randomised phase III trial. *Lancet* **373**, 1525–1531 (2009).
4. H. Kimura, K. Sakai, T. Arao, T. Shimoyama, T. Tamura, K. Nishio, Antibody-dependent cellular cytotoxicity of cetuximab against tumor cells with wild-type or mutant epidermal growth factor receptor. *Cancer Sci.* **98**, 1275–1280 (2007).
5. E. Van Cutsem, C. H. Köhne, E. Hitre, J. Zaluski, C. R. Chang Chien, A. Makhson, G. D'Haens, T. Pintér, R. Lim, G. Bodoky, J. K. Roh, G. Folprecht, P. Ruff, C. Stroh, S. Tejpar, M. Schlichting, J. Nippgen, P. Rougier, Cetuximab and chemotherapy as initial treatment for metastatic colorectal cancer. *N. Engl. J. Med.* **360**, 1408–1417 (2009).
6. C. Bokemeyer, I. Bondarenko, A. Makhson, J. T. Hartmann, J. Aparicio, F. de Braud, S. Donea, H. Ludwig, G. Schuch, C. Stroh, A. H. Loos, A. Zubel, P. Koralewski, Fluorouracil, leucovorin, and oxaliplatin with and without cetuximab in the first-line treatment of metastatic colorectal cancer. *J. Clin. Oncol.* **27**, 663–671 (2009).
7. J. Tol, M. Koopman, A. Cats, C. J. Rodenburg, G. J. Creemers, J. G. Schrama, F. L. Erdkamp, A. H. Vos, C. J. van Groeningen, H. A. Sinnige, D. J. Richel, E. E. Voest, J. R. Dijkstra, M. E. Vink-Börger, N. F. Antonini, L. Mol, J. H. van Krieken, O. Dalesio, C. J. Punt, Chemotherapy, bevacizumab, and cetuximab in metastatic colorectal cancer. *N. Engl. J. Med.* **360**, 563–572 (2009).
8. C. J. Allegra, J. M. Jessup, M. R. Somerfield, S. R. Hamilton, E. H. Hammond, D. F. Hayes, P. K. McAllister, R. F. Morton, R. L. Schilsky, American Society of Clinical Oncology provisional clinical opinion: Testing for *KRAS* gene mutations in patients with metastatic colorectal carcinoma to predict response to anti-epidermal growth factor receptor monoclonal antibody therapy. *J. Clin. Oncol.* **27**, 2091–2096 (2009).
9. F. Di Nicolantonio, M. Martini, F. Molinari, A. Sartore-Bianchi, S. Arena, P. Saletti, S. De Dosso, L. Mazzucchelli, M. Frattini, S. Siena, A. Bardelli, Wild-type *BRAF* is required for response to panitumumab or cetuximab in metastatic colorectal cancer. *J. Clin. Oncol.* **26**, 5705–5712 (2008).
10. W. De Roock, B. Claes, D. Bernasconi, J. De Schutter, B. Biesmans, G. Fountzilas, K. T. Kalogeras, V. Kotoula, D. Papamichael, P. Laurent-Puig, F. Penault-Llorca, P. Rougier, B. Vincenzi, D. Santini, G. Tonini, F. Cappuzzo, M. Frattini, F. Molinari, P. Saletti, S. De Dosso, M. Martini, A. Bardelli, S. Siena, A. Sartore-Bianchi, J. Tabernero, T. Macarulla, F. Di Fiore, A. O. Gangloff, F. Ciardiello, P. Pfeiffer, C. Qvortrup, T. P. Hansen, E. Van Cutsem, H. Piessevaux, D. Lambrechts, M. Delorenzi, S. Tejpar, Effects of *KRAS*, *BRAF*, *NRAS*, and *PIK3CA* mutations on the efficacy of cetuximab plus chemotherapy in chemotherapy-refractory metastatic colorectal cancer: A retrospective consortium analysis. *Lancet Oncol.* **11**, 753–762 (2010).
11. C. S. Karapetis, S. Khambata-Ford, D. J. Jonker, C. J. O'Callaghan, D. Tu, N. C. Tebbutt, R. J. Simes, H. Chalchal, J. D. Shapiro, S. Robitaille, T. J. Price, L. Shepherd, H. J. Au, C. Langer, M. J. Moore, J. R. Zalcberg, *K-ras* mutations and benefit from cetuximab in advanced colorectal cancer. *N. Engl. J. Med.* **359**, 1757–1765 (2008).
12. J. A. Engelman, K. Zejnullahu, T. Mitsudomi, Y. Song, C. Hyland, J. O. Park, N. Lindeman, C. M. Gale, X. Zhao, J. Christensen, T. Kosaka, A. J. Holmes, A. M. Rogers, F. Cappuzzo, T. Mok, C. Lee, B. E. Johnson, L. C. Cantley, P. A. Jänne, *MET* amplification leads to gefitinib resistance in lung cancer by activating ERBB3 signaling. *Science* **316**, 1039–1043 (2007).
13. J. A. Engelman, T. Mukohara, K. Zejnullahu, E. Lifshits, A. M. Borrás, C. M. Gale, G. N. Naumov, B. Y. Yeap, E. Jarrell, J. Sun, S. Tracy, X. Zhao, J. V. Heymach, B. E. Johnson, L. C. Cantley, P. A. Jänne, Allelic dilution obscures detection of a biologically significant resistance mutation in *EGFR*-amplified lung cancer. *J. Clin. Invest.* **116**, 2695–2706 (2006).
14. T. Mukohara, J. A. Engelman, N. H. Hanna, B. Y. Yeap, S. Kobayashi, N. Lindeman, B. Halmos, J. Pearlberg, Z. Tsuchihashi, L. C. Cantley, D. G. Tenen, B. E. Johnson, P. A. Jänne, Differential effects of gefitinib and cetuximab on non–small-cell lung cancers bearing epidermal growth factor receptor mutations. *J. Natl. Cancer Inst.* **97**, 1185–1194 (2005).
15. J. Baselga, D. Pfister, M. R. Cooper, R. Cohen, B. Burtness, M. Bos, G. D'Andrea, A. Seidman, L. Norton, K. Gunnett, J. Falcey, V. Anderson, H. Waksal, J. Mendelsohn, Phase I studies of anti–epidermal growth factor receptor chimeric antibody C225 alone and in combination with cisplatin. *J. Clin. Oncol.* **18**, 904–914 (2000).
16. A. B. Turke, K. Zejnullahu, Y. L. Wu, Y. Song, D. Dias-Santagata, E. Lifshits, L. Toschi, A. Rogers, T. Mok, L. Sequist, N. I. Lindeman, C. Murphy, S. Akhavanfard, B. Y. Yeap, Y. Xiao, M. Capelletti, A. J. Iafrate, C. Lee, J. G. Christensen, J. A. Engelman, P. A. Jänne, Preexistence and clonal selection of *MET* amplification in *EGFR* mutant NSCLC. *Cancer Cell* **17**, 77–88 (2010).
17. K. Yonesaka, K. Zejnullahu, N. Lindeman, A. J. Homes, D. M. Jackman, F. Zhao, A. M. Rogers, B. E. Johnson, P. A. Jänne, Autocrine production of amphiregulin predicts sensitivity to both gefitinib and cetuximab in *EGFR* wild-type cancers. *Clin. Cancer Res.* **14**, 6963–6973 (2008).
18. S. Li, A. D. Couvillon, B. B. Brasher, R. A. Van Etten, Tyrosine phosphorylation of Grb2 by Bcr/Abl and epidermal growth factor receptor: A novel regulatory mechanism for tyrosine kinase signaling. *EMBO J.* **20**, 6793–6804 (2001).

Downloaded from stm.sciencemag.org on February 25, 2012

19. J. Baselga, S. M. Swain, Novel anticancer targets: Revisiting ERBB2 and discovering ERBB3. *Nat. Rev. Cancer* **9**, 463–475 (2009).
20. J. A. Engelman, P. A. Jänne, C. Mermel, J. Pearlberg, T. Mukohara, C. Fleet, K. Cichowski, B. E. Johnson, L. C. Cantley, ErbB-3 mediates phosphoinositide 3-kinase activity in gefitinib-sensitive non-small cell lung cancer cell lines. *Proc. Natl. Acad. Sci. U.S.A.* **102**, 3788–3793 (2005).
21. M. C. Franklin, K. D. Carey, F. F. Vajdos, D. J. Leahy, A. M. de Vos, M. X. Sliwkowski, Insights into ErbB signaling from the structure of the ErbB2-pertuzumab complex. *Cancer Cell* **5**, 317–328 (2004).
22. L. V. Sequist, R. G. Martins, D. Spigel, S. M. Grunberg, A. Spira, P. A. Jänne, V. A. Joshi, D. McCollum, T. L. Evans, A. Muzikansky, G. L. Kuhlmann, M. Han, J. S. Goldberg, J. Settleman, A. J. Iafrate, J. A. Engelman, D. A. Haber, B. E. Johnson, T. J. Lynch, First-line gefitinib in patients with advanced non–small-cell lung cancer harboring somatic *EGFR* mutations. *J. Clin. Oncol.* **26**, 2442–2449 (2008).
23. R. S. Finn, R. Gagnon, A. Di Leo, M. F. Press, M. Arbushites, M. Koehler, Prognostic and predictive value of HER2 extracellular domain in metastatic breast cancer treated with lapatinib and paclitaxel in a randomized phase III study. *J. Clin. Oncol.* **27**, 5552–5558 (2009).
24. M. N. Fornier, A. D. Seidman, M. K. Schwartz, F. Ghani, R. Thiel, L. Norton, C. Hudis, Serum HER2 extracellular domain in metastatic breast cancer patients treated with weekly trastuzumab and paclitaxel: Association with HER2 status by immunohistochemistry and fluorescence in situ hybridization and with response rate. *Ann. Oncol.* **16**, 234–239 (2005).
25. T. O'Hare, W. C. Shakespeare, X. Zhu, C. A. Eide, V. M. Rivera, F. Wang, L. T. Adrian, T. Zhou, W. S. Huang, Q. Xu, C. A. Metcalf III, J. W. Tyner, M. M. Loriaux, A. S. Corbin, S. Wardwell, Y. Ning, J. A. Keats, Y. Wang, R. Sundaramoorthi, M. Thomas, D. Zhou, J. Snodgrass, L. Commodore, T. K. Sawyer, D. C. Dalgarno, M. W. Deininger, B. J. Druker, T. Clackson, AP24534, a pan-BCR-ABL inhibitor for chronic myeloid leukemia, potently inhibits the T315I mutant and overcomes mutation-based resistance. *Cancer Cell* **16**, 401–412 (2009).
26. H. Kantarjian, N. P. Shah, A. Hochhaus, J. Cortes, S. Shah, M. Ayala, B. Moiraghi, Z. Shen, J. Mayer, R. Pasquini, H. Nakamae, F. Huguet, C. Boqué, C. Chuah, E. Bleickardt, M. B. Bradley-Garelik, C. Zhu, T. Szatrowski, D. Shapiro, M. Baccarani, Dasatinib versus imatinib in newly diagnosed chronic-phase chronic myeloid leukemia. *N. Engl. J. Med.* **362**, 2260–2270 (2010).
27. S. Kobayashi, T. J. Boggon, T. Dayaram, P. A. Jänne, O. Kocher, M. Meyerson, B. E. Johnson, M. J. Eck, D. G. Tenen, B. Halmos, *EGFR* mutation and resistance of non–small-cell lung cancer to gefitinib. *N. Engl. J. Med.* **352**, 786–792 (2005).
28. W. Pao, V. A. Miller, K. A. Politi, G. J. Riely, R. Somwar, M. F. Zakowski, M. G. Kris, H. Varmus, Acquired resistance of lung adenocarcinomas to gefitinib or erlotinib is associated with a second mutation in the EGFR kinase domain. *PLoS Med.* **2**, e73 (2005).
29. D. L. Wheeler, S. Huang, T. J. Kruser, M. M. Nechrebecki, E. A. Armstrong, S. Benavente, V. Gondi, K. T. Hsu, P. M. Harari, Mechanisms of acquired resistance to cetuximab: Role of HER (ErbB) family members. *Oncogene* **27**, 3944–3956 (2008).
30. B. Schoeberl, A. C. Faber, D. Li, M. C. Liang, K. Crosby, M. Onsum, O. Burenkova, E. Pace, Z. Walton, L. Nie, A. Fulgham, Y. Song, U. B. Nielsen, J. A. Engelman, K. K. Wong, An ErbB3 antibody, MM-121, is active in cancers with ligand-dependent activation. *Cancer Res.* **70**, 2485–2494 (2010).
31. C. A. Ritter, M. Perez-Torres, C. Rinehart, M. Guix, T. Dugger, J. A. Engelman, C. L. Arteaga, Human breast cancer cells selected for resistance to trastuzumab in vivo overexpress epidermal growth factor receptor and ErbB ligands and remain dependent on the ErbB receptor network. *Clin. Cancer Res.* **13**, 4909–4919 (2007).
32. M. P. Piechocki, G. H. Yoo, S. K. Dibbley, F. Lonardo, Breast cancer expressing the activated HER2/neu is sensitive to gefitinib in vitro and in vivo and acquires resistance through a novel point mutation in the HER2/neu. *Cancer Res.* **67**, 6825–6843 (2007).
33. F. Ciardiello, R. Bianco, V. Damiano, S. De Lorenzo, S. Pepe, S. De Placido, Z. Fan, J. Mendelsohn, A. R. Bianco, G. Tortora, Antitumor activity of sequential treatment with topotecan and anti-epidermal growth factor receptor monoclonal antibody C225. *Clin. Cancer Res.* **5**, 909–916 (1999).
34. J. Albanell, J. Codony-Servat, F. Rojo, J. M. Del Campo, S. Sauleda, J. Anido, G. Raspall, J. Giralt, J. Roselló, R. I. Nicholson, J. Mendelsohn, J. Baselga, Activated extracellular signal-regulated kinases: Association with epidermal growth factor receptor/transforming growth factor α expression in head and neck squamous carcinoma and inhibition by anti-epidermal growth factor receptor treatments. *Cancer Res.* **61**, 6500–6510 (2001).
35. X. Zhao, B. A. Weir, T. LaFramboise, M. Lin, R. Beroukhim, L. Garraway, J. Beheshti, J. C. Lee, K. Naoki, W. G. Richards, D. Sugarbaker, F. Chen, M. A. Rubin, P. A. Jänne, L. Girard, J. Minna, D. Christiani, C. Li, W. R. Sellers, M. Meyerson, Homozygous deletions and chromosome amplifications in human lung carcinomas revealed by single nucleotide polymorphism array analysis. *Cancer Res.* **65**, 5561–5570 (2005).
36. W. Zhou, D. Ercan, L. Chen, C. H. Yun, D. Li, M. Capelletti, A. B. Cortot, L. Chirieac, R. E. Iacob, R. Padera, J. R. Engen, K. K. Wong, M. J. Eck, N. S. Gray, P. A. Jänne, Novel mutant-selective EGFR kinase inhibitors against EGFR T790M. *Nature* **462**, 1070–1074 (2009).
37. S. M. Rothenberg, J. A. Engelman, S. Le, D. J. Riese II, D. A. Haber, J. Settleman, Modeling oncogene addiction using RNA interference. *Proc. Natl. Acad. Sci. U.S.A.* **105**, 12480–12484 (2008).
38. J. A. Engelman, K. Zejnullahu, C. M. Gale, E. Lifshits, A. J. Gonzales, T. Shimamura, F. Zhao, P. W. Vincent, G. N. Naumov, J. E. Bradner, I. W. Althaus, L. Gandhi, G. I. Shapiro, J. M. Nelson, J. V. Heymach, M. Meyerson, K. K. Wong, P. A. Jänne, PF00299804, an irreversible pan-ERBB inhibitor, is effective in lung cancer models with *EGFR* and *ERBB2* mutations that are resistant to gefitinib. *Cancer Res.* **67**, 11924–11932 (2007).

39. **Acknowledgments:** We thank F. Zhao for technical assistance. **Funding:** Supported by NIH grants RO1CA114465 (P.A.J.), R01CA135257 (P.A.J. and J.A.E.), and P50 CA58187 (M.V.-G.); American Cancer Society RSG0610201CCE (P.A.J. and J.A.E.); the Lung Cancer SPORE P50 CA090578 (P.A.J. and J.A.E.); the Gastrointestinal Cancer SPORE P50 CA127003 (P.A.J. and J.A.E.); the William Randolph Hearst Foundation (R.A.S.); the Hazel and Samuel Bellin research fund (P.A.J.); and Cammarata Family Foundation Research Fund (P.A.J.). **Author contributions:** K.Y., K. Nakagawa, and P.A.J. designed the studies. K.Y., K.Z., D.E., A.R., J. Souglakos, T.O., J. Sun, and J. Swanson performed laboratory assays and analyses. K.Y., I.O., T. Satoh, F.C., M.R., M. Takeda, Y.F., J.P., T. Shimizu, O.M., A.D., K. Taira, K. Takeda, H.I., M. Takada, K.O., R.A.S., M.F., and K. Nishio identified and provided clinical data on cetuximab-treated patients, performed genotyping and analyses, and analyzed tumor and plasma heregulin levels. K.Y., E.L., and J.A.E. carried out in vivo analyses. Y.C. and M.V.-G. performed FISH analyses. K.Y., K. Nakagawa, and P.A.J. wrote the paper. **Competing interests:** P.A.J. has consulted for Genentech and Roche. J.A.E. has consulted for Roche and Bristol-Myers Squibb. T. Satoh has consulted for Merck-Serono, Bristol-Myers Squib, Chugai-Pharmaceuticals, Takeda, Sanofi-Aventis, Taiho Pharmaceutical, Pfizer, and Daiichi-Sankyo P.A.J. and J.A.E. have received royalties from Roche on intellectual property not related to this work. A patent has been filed by Dana-Farber Cancer Institute involving the use of MET and EGFR inhibitors to overcome resistance to EGFR inhibitors. **Accession numbers:** The SNP data have been deposited at the Gene Expression Omnibus (GEO) database with accession number GSE30255.

Submitted 25 March 2011
Accepted 15 July 2011
Published 7 September 2011
10.1126/scitranslmed.3002442

Citation: K. Yonesaka, K. Zejnullahu, I. Okamoto, T. Satoh, F. Cappuzzo, J. Souglakos, D. Ercan, A. Rogers, M. Roncalli, M. Takeda, Y. Fujisaka, J. Philips, T. Shimizu, O. Maenishi, Y. Cho, J. Sun, A. Destro, K. Taira, K. Takeda, T. Okabe, J. Swanson, H. Itoh, M. Takada, E. Lifshits, K. Okuno, J. A. Engelman, R. A. Shivdasani, K. Nishio, M. Fukuoka, M. Varella-Garcia, K. Nakagawa, P. A. Jänne, Activation of ERBB2 signaling causes resistance to the EGFR-directed therapeutic antibody cetuximab. *Sci. Transl. Med.* **3**, 99ra86 (2011).

Downloaded from stm.sciencemag.org on February 25, 2012

British Journal of Cancer (2011) 105, 807–813
© 2011 Cancer Research UK All rights reserved 0007–0920/11
www.bjcancer.com

Differential roles of trans-phosphorylated EGFR, HER2, HER3, and RET as heterodimerisation partners of MET in lung cancer with *MET* amplification

J Tanizaki[1], I Okamoto[*,1], K Sakai[2] and K Nakagawa[1]

[1]Department of Medical Oncology, Kinki University Faculty of Medicine, 377-2 Ohno-higashi, Osaka-Sayama, Osaka 589-8511, Japan; [2]Genome Biology, Kinki University Faculty of Medicine, 377-2 Ohno-higashi, Osaka-Sayama, Osaka 589-8511, Japan

BACKGROUND: MET is a receptor tyrosine kinase (RTK) whose gene is amplified in various tumour types. We investigated the roles and mechanisms of RTK heterodimerisation in lung cancer with *MET* amplification.

METHODS: With the use of an RTK array, we identified phosphorylated RTKs in lung cancer cells with *MET* amplification. We examined the roles and mechanisms of action of these RTKs with immunoprecipitation, annexin V binding, and cell migration assays.

RESULTS: We identified epidermal growth factor receptor (EGFR), human EGFR (HER)2, HER3, and RET in addition to MET as highly phosphorylated RTKs in lung cancer cells with *MET* amplification. Immunoprecipitation revealed that EGFR, HER2, HER3, and RET each formed a heterodimer exclusively with MET and that these associations were markedly reduced in extent by treatment with a MET kinase inhibitor. RNA interference-mediated depletion of EGFR, HER2, or HER3 induced apoptosis in association with inhibition of AKT and ERK signalling pathways, whereas depletion of HER2 or RET inhibited both cell migration and STAT3 signalling.

CONCLUSION: Our data suggest that heterodimers of MET with EGFR, HER2, HER3, or RET have differential roles in tumour development, and they provide new insight into the function of trans-phosphorylated RTKs as heterodimerisation partners of MET in lung cancer with *MET* amplification.

British Journal of Cancer (2011) **105,** 807–813. doi:10.1038/bjc.2011.322 www.bjcancer.com
Published online 16 August 2011
© 2011 Cancer Research UK

Keywords: *MET* amplification; trans-phosphorylation; heterodimerisation; lung cancer

The proto-oncogene *MET* encodes a receptor tyrosine kinase (RTK). Amplification of *MET* occurs in a subset of solid tumour types, with aberrant MET signalling having been implicated in cell proliferation and survival as well as in cell migration and invasiveness (Trusolino and Comoglio, 2002; Birchmeier *et al*, 2003). Tumours with *MET* amplification are highly dependent on MET signalling for their progression, and several small-molecule inhibitors of MET have been developed and found to manifest marked antitumour efficacy both *in vitro* and *in vivo* (Smolen *et al*, 2006; Lutterbach *et al*, 2007; Okamoto *et al*, 2010). Such inhibitors are now undergoing clinical trials in humans.

Lung cancer is the leading cause of cancer mortality worldwide. Molecularly targeted agents, such as epidermal growth factor receptor (EGFR)–tyrosine kinase inhibitors (TKIs), have been found to provide substantial clinical benefit in lung cancer patients (Asahina *et al*, 2006; Sequist *et al*, 2008; Kwak *et al*, 2010), and MET is considered a molecular target of potential relevance to lung cancer. Amplification of *MET* occurs in ~4% of lung cancer patients, with activation of MET signalling being associated with advanced cancer stage and shorter patient survival (Masuya *et al*, 2004; Zhao *et al*, 2005; Nakamura *et al*, 2007). MET–TKIs are currently undergoing early-phase clinical testing in lung cancer patients. Optimisation of the clinical efficacy of such drugs will require further characterisation of MET signal transduction in tumours with *MET* amplification. Although MET has been found to associate with other RTKs (Jo *et al*, 2000; Engelman *et al*, 2007; Lai *et al*, 2009; Mueller *et al*, 2010), the underlying mechanisms and regulation of such association in lung cancer with *MET* amplification remain largely unclear.

We have now shown that several RTKs, including EGFR, human EGFR (HER)2, HER3, and RET in addition to MET, are highly phosphorylated in *MET* amplification-positive lung cancer cells, and that these RTKs form heterodimers with MET. Such heterodimerisation results in trans-phosphorylation of these RTKs in a manner dependent on the kinase activity of MET. We further investigated the functional roles of these RTKs in lung cancer cells with *MET* amplification.

MATERIALS AND METHODS

Cell culture and reagents

The human non-small cell lung cancer (NSCLC) cell lines H1993, PC9, and HCC827, the human breast cancer cell lines SK-BR3 and BT-474, and the human medullary thyroid carcinoma cell line TT were obtained from American Type Culture Collection (Manassas, VA, USA). The human NSCLC cell line EBC-1 was obtained from the Health Science Research Resources Bank (Tokyo, Japan). SK-BR3 cells were cultured in McCoy's medium (Invitrogen,

*Correspondence: Dr I Okamoto; E-mail: chi-okamoto@dotd.med.kindai.ac.jp
Received 18 April 2011; revised 24 June 2011; accepted 21 July 2011; published online 16 August 2011

Carlsbad, CA, USA) supplemented with 10% fetal bovine serum (FBS); BT-474 cells in Dulbecco's modified Eagle's medium (Invitrogen) supplemented with 10% FBS; TT cells in Ham's F-12 medium (Sigma, St Louis, MO, USA) supplemented with 10% FBS; and other cells in RPMI 1640 medium (Sigma) supplemented with 10% FBS. All cell lines were maintained under a humidified atmosphere of 5% CO_2 at 37 °C. PHA-665752 was obtained from Tocris Bioscience (Bristol, UK), gefitinib was from Kemprotec (Middlesbrough, UK), lapatinib was from Sequoia Research Products (Pangbourne, UK), and vandetanib was from ShangHai Biochempartner (Shanghai, China).

RTK array analysis

Tyrosine-phosphorylated RTKs were detected with the use of Array 001 (R&D Systems, Minneapolis, MN, USA), which contains capture antibodies to 42 RTKs in duplicate wells. Cell lysates were incubated overnight at 4 °C with the array in the provided buffer. Target RTKs are captured by the respective capture antibodies, and tyrosine-phosphorylated RTKs are subsequently detected with horseradish peroxidase-conjugated antibodies to phosphotyrosine.

Immunoblot analysis

Cells were washed twice with ice-cold phosphate-buffered saline (PBS) and then lysed in a solution containing 20 mM Tris-HCl (pH 7.5), 150 mM NaCl, 1 mM EDTA, 1% Triton X-100, 2.5 mM sodium pyrophosphate, 1 mM phenylmethylsulfonyl fluoride, and leupeptin (1 $\mu g\,ml^{-1}$). The protein concentration of cell lysates was determined with the use of a BCA protein assay kit (Thermo Fischer Scientific, Waltham, MA, USA), and equal amounts of lysate protein were subjected to SDS–polyacrylamide gel electrophoresis on a 7.5 or 12% gel (Bio-Rad, Hercules, CA, USA). The separated proteins were transferred to a nitrocellulose membrane, which was then incubated with Blocking One solution (Nacalai Tesque, Kyoto, Japan) for 20 min at room temperature before incubation overnight at 4 °C with primary antibodies. Rabbit polyclonal antibodies to phosphorylated human MET (pY1234/pY1235), to phosphorylated EGFR (pY1068), to phosphorylated HER2 (pY1221), to phosphorylated HER3 (pY1289), to phosphorylated RET (pY905), to AKT, to phosphorylated AKT, to signal transducer and activator of transcription 3 (STAT3), to phosphorylated STAT3, and to poly(ADP-ribose) polymerase (PARP) were obtained from Cell Signaling Technology (Danvers, MA, USA); those to HER3, to RET, to extracellular signal-regulated kinase (ERK), and to phosphorylated ERK were from Santa Cruz Biotechnology (Santa Cruz, CA, USA); those to MET were from Zymed (South San Francisco, CA, USA); those to HER2 were from Millipore (Billerica, MA, USA); and those to β-actin were from Sigma. Mouse monoclonal antibodies to EGFR were obtained from Invitrogen. All antibodies were used at a 1 : 1000 dilution, with the exception of those to β-actin (1 : 200) and to EGFR (1 : 100). After incubation with primary antibodies, the membrane was washed with PBS containing 0.05% Tween 20 before incubation for 1 h at room temperature with horseradish peroxidase-conjugated goat antibodies to rabbit or mouse immunoglobulin (Ig) G (Sigma). Immune complexes were finally detected with chemiluminescence reagents (GE Healthcare, Little Chalfont, UK).

Immunoprecipitation

Total cell lysates (800 μg of protein) were incubated overnight at 4 °C either with antibodies to MET (Cell Signaling), to EGFR (Cell Signaling), to HER2 (Cell Signaling), to HER3 (Santa Cruz Biotechnology), or to RET (Santa Cruz Biotechnology) or with control IgG (Cell Signaling). Immune complexes were then precipitated by further incubation for 1 h at 4 °C with a suspension of protein G- and protein A-conjugated agarose (Calbiochem, Darmstadt, Germany). Immunoprecipitates were isolated, washed, resolved by SDS–polyacrylamide gel electrophoresis on a 7.5% gel, and subjected to immunoblot analysis as described above.

Gene silencing

Cells were plated at 50–60% confluence in six-well plates or 25-cm^2 flasks and then incubated for 24 h before transient transfection for the indicated times with small interfering RNAs (siRNAs) mixed with the Lipofectamine reagent (Invitrogen). The siRNAs specific for MET (MET-1, 5′-ACAAGAUCGUCAACAAAAA-3′; MET-2, 5′-CUACAGAAAUGGUUUCAAA-3′), EGFR (EGFR-1, 5′-GAAAUAUGUACUACGAAA-3′; EGFR-2, 5′-GGAACUGGAUAUUCUGAAA-3′), HER2 (HER2-1, 5′-CCAUUGAUGUCUACAUGAU-3′; HER2-2, 5′-AGGACAUCUUCCACAAGAA-3′), HER3 (HER3-1, 5′-UCUUCGUCAUGUUGAACUA-3′; HER3-2, 5′-CCUCCUUGAUGAUGACCCA-3′), or RET (RET-1, 5′-GGGAUGCUUACUGGGAGAA-3′; RET-2, 5′-CCACCCACAUGUCAUCAAA-3′) mRNAs as well as nonspecific (control) siRNAs were obtained from Nippon EGT (Toyama, Japan). The data presented were obtained with MET-1, EGFR-1, HER2-1, HER3-1, and RET-1 siRNAs, but similar results were obtained with MET-2, EGFR-2, HER2-2, HER3-2, and RET-2.

Cell proliferation assay

Cells were transferred to 96-well flat-bottomed plates and cultured for 24 h before exposure to various agents or transfection with siRNAs for 72 h. TetraColor One (5 mM tetrazolium monosodium salt and 0.2 mM 1-methoxy-5-methyl phenazinium methylsulphate; Seikagaku, Tokyo, Japan) was then added to each well, and the cells were incubated for 3 h at 37 °C before measurement of absorbance at 490 nm with a Multiskan Spectrum instrument (Thermo Labsystems, Boston, MA, USA). Absorbance values were expressed as a percentage of that for control cells.

Annexin V-binding assay

Binding of annexin V to cells was measured with the use of an annexin-V-FLUOS Staining Kit (Roche, Basel, Switzerland). Cells were harvested by exposure to trypsin-EDTA, washed with PBS, and centrifuged at 200 × g for 5 min. The cell pellets were resuspended in 100 μl of annexin-V-FLUOS labelling solution, incubated for 10–15 min at 15–25 °C, and then analysed for fluorescence with a flow cytometer (FACSCalibur, Becton Dickinson, Franklin Lakes, NJ, USA) and Cell Quest software (Becton Dickinson).

Cell migration assay

Cells were transfected with siRNAs specific for MET, EGFR HER2, HER3, or RET mRNAs for 24 h and were then transferred in serum-free medium to cell culture inserts (pore size, 8 μm; BD Falcon, Franklin Lakes, NJ, USA) of a transwell apparatus. Complete medium (containing 10% FBS) served as the chemoattractant in the lower chamber. After culture for 24 h, cells that had migrated through the membrane pores were fixed and stained. Cell migration was quantified by counting the numbers of cells in five randomly chosen microscopic fields of view (magnification, × 400) per membrane, and the mean value was then expressed relative to that for cells transfected with a control siRNA.

RESULTS

EGFR, HER2, HER3, and RET are highly phosphorylated in a manner dependent on MET kinase activity in lung cancer cell lines with *MET* amplification

We first examined the phosphorylation of RTKs in lung cancer cells positive for *MET* amplification. With the use of an RTK array,

© 2011 Cancer Research UK

we found that EBC-1 and H1993, two human lung cancer cell lines with *MET* amplification, exhibited a high level of tyrosine phosphorylation of MET, EGFR, HER2, HER3, and RET under conditions of serum deprivation (Figure 1A). The MET inhibitor PHA-665752 markedly reduced the level of MET phosphorylation as well as that of EGFR, HER2, HER3, and RET phosphorylation (Figure 1A). Consistent with these results obtained with the RTK array, immunoblot analysis showed that PHA-665752 inhibited the phosphorylation of MET, EGFR, HER2, HER3, and RET as well as that of the downstream signalling molecules AKT, ERK, and STAT3 in both EBC-1 and H1993 cells (Figure 1B). To investigate whether the observed phosphorylation of these RTKs is mediated by the corresponding intrinsic kinase activities, we examined the effects of various TKIs. The EGFR–TKI gefitinib had little effect on the phosphorylation of EGFR or that of AKT, ERK, or STAT3 in EBC-1 or H1993 cells (Figure 1B), whereas it markedly inhibited the phosphorylation of these molecules in *EGFR* mutation-positive lung cancer cell lines (PC9 and HCC827) that manifest constitutive activation of the EGFR kinase (Figure 1C, data not shown). Neither lapatinib (a dual TKI of EGFR and HER2) nor vandetanib

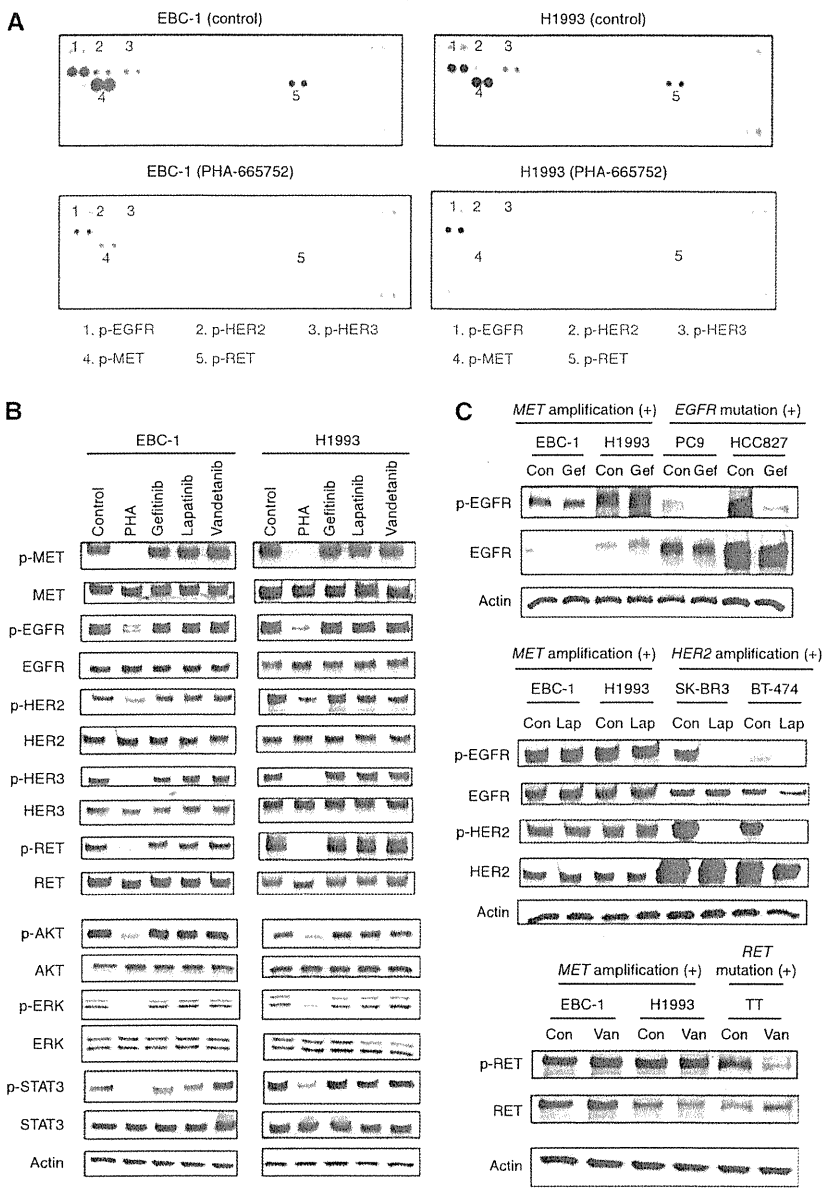

Figure 1 Phosphorylation of multiple RTKs in lung cancer cells with *MET* amplification. (**A**) EBC-1 and H1993 cells were deprived of serum for 24 h and then incubated for 2 h in the absence (control) or presence of PHA-665752 (500 nM). Cell lysates were prepared and incubated with an RTK array for determination of the phosphorylation status of each enzyme. Each RTK is spotted in duplicate, and the pairs of dots in each corner of the array are positive controls. The numbered pairs of dots correspond to the indicated phosphorylated (p-) RTKs. (**B**) EBC-1 and H1993 cells were deprived of serum for 24 h and then incubated for 2 h in the absence or presence of PHA-665752 (PHA, 500 nM), gefitinib (1 μM), lapatinib (1 μM), or vandetanib (1 μM), after which cell lysates were subjected to immunoblot analysis with antibodies to phosphorylated or total forms of MET, EGFR, HER2, HER3, RET, AKT, ERK, or STAT3 or with those to β-actin (loading control). (**C**) The indicated cell lines were deprived of serum for 24 h and then incubated for 2 h in the absence (Con) or presence of gefitinib (Gef, 1 μM), lapatinib (Lap, 1 μM), or vandetanib (Van, 1 μM), after which cell lysates were subjected to immunoblot analysis with antibodies to the indicated proteins.

© 2011 Cancer Research UK

(a TKI of RET) had a substantial effect on the phosphorylation of any of the RTKs or their downstream signalling molecules in EBC-1 or H1993 cells (Figure 1B), whereas these drugs inhibited their specific target RTKs in *HER2* amplification-positive breast cancer cell lines (SK-BR3 and BT-474) or *RET* mutation-positive medullary thyroid carcinoma TT cells, respectively (Figure 1C). These data thus suggested that phosphorylation of MET, EGFR, HER2, HER3, and RET as well as that of the downstream signalling molecules is dependent on the kinase activity of MET, but is independent of that of the other RTKs, in *MET* amplification-positive lung cancer cells.

EGFR, HER2, HER3, and RET associate with MET in lung cancer cells with *MET* amplification

To investigate further the mechanism of EGFR, HER2, HER3, and RET phosphorylation in *MET* amplification-positive cells, we examined the interactions among these RTKs by immunoprecipitation analysis. MET was immunoprecipitated from EBC-1 and H1993 cell lysates, and the resulting precipitates were subjected to immunoblot analysis with antibodies to MET, to EGFR, to HER2, to HER3, and to RET. EGFR, HER2, HER3, and RET co-precipitated with MET from both cell lines, and the extent of these associations was markedly reduced by prior treatment of the cells with PHA-665752 (Figure 2A). Reciprocal immunoprecipitation analysis further revealed that MET, but not HER2, HER3, or RET, co-precipitated with EGFR and that only MET co-precipitated with HER2, HER3, or RET (Figure 2B). These data thus suggested that phosphorylation of EGFR, HER2, HER3, and RET in *MET* amplification-positive lung cancer cells is mediated through interaction of these RTKs with MET.

Effects of TKIs on cell proliferation and apoptosis in lung cancer cells with *MET* amplification

To examine the roles of MET, EGFR, HER2, HER3, and RET in lung cancer cells with *MET* amplification, we first investigated the effects of PHA-665752, gefitinib, lapatinib, and vandetanib on cell proliferation and survival. PHA-665752 inhibited the proliferation of EBC-1 and H1993 cells, whereas gefitinib, lapatinib, and vandetanib had no such effect (Figure 3A), consistent with our findings that AKT, ERK, and STAT3 signalling pathways are not dependent on the kinase activity of EGFR, HER2, or RET in these cells (Figure 1B). We further found that PHA-665752, but not gefitinib, lapatinib, or vandetanib, induced marked apoptosis in EBC-1 and H1993 cells (Figure 3B). A substantial level of PARP cleavage, a characteristic of apoptosis, was also apparent only in the cells treated with PHA-665752 (Figure 3C). These results thus

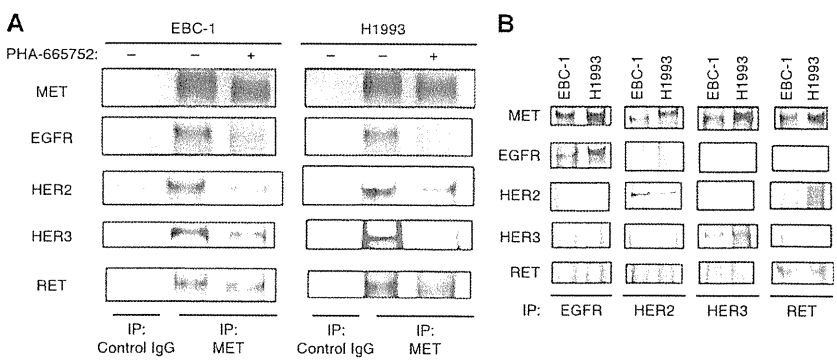

Figure 2 Association of MET with EGFR, HER2, HER3, and RET in lung cancer cells positive for *MET* amplification. (**A**) Serum-deprived EBC-1 and H1993 cells were incubated for 2 h in the absence or presence of PHA-665752 (500 nM), lysed, and subjected to immunoprecipitation (IP) with antibodies to MET or control IgG. The resulting precipitates were subjected to immunoblot analysis with antibodies to the indicated proteins. (**B**) Serum-deprived cells were lysed and subjected to IP with antibodies to EGFR, to HER2, to HER3, or to RET, and the resulting precipitates were subjected to immunoblot analysis with antibodies to the indicated proteins.

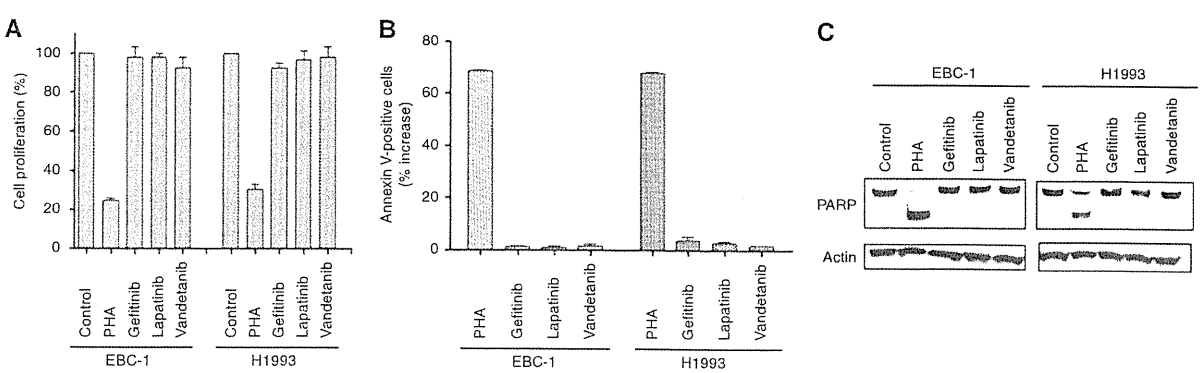

Figure 3 Effects of various TKIs on cell proliferation and apoptosis in lung cancer cells with *MET* amplification. (**A**) EBC-1 and H1993 cells were cultured for 72 h in complete medium with or without PHA-665752 (500 nM), gefitinib (1 μM), lapatinib (1 μM), or vandetanib (1 μM), after which the number of viable cells was determined. Absorbance values were expressed as a percentage of that for untreated cells (control). Data are means ± s.e. from three independent experiments. (**B**) Cells were incubated for 72 h as in (**A**), after which the number of apoptotic cells was determined by staining with annexin V and propidium iodide followed by flow cytometry. Data are expressed as the percentage increase in the number of annexin V-positive cells relative to the corresponding value for cells incubated without agent and are means ± s.e. from three independent experiments. (**C**) Cells incubated as in (**A**) were lysed and subjected to immunoblot analysis with antibodies to PARP and to β-actin.

© 2011 Cancer Research UK

suggested that only the MET–TKI induced apoptosis, resulting in inhibition of cell growth, in *MET* amplification-positive cells.

Effects of depletion of MET, EGFR, HER2, HER3, or RET on cell proliferation, apoptosis, and migration in *MET* amplification-positive lung cancer cells

With the use of specific siRNAs, we next depleted EBC-1 and H1993 cells of MET, EGFR, HER2, HER3, or RET. Immunoblot analysis confirmed that transfection of cells with each siRNA resulted in the marked and selective depletion of the targeted RTK (Figure 4A). Phosphorylation of AKT and ERK was inhibited by depletion of MET, EGFR, HER2, or HER3, but not by that of RET, whereas phosphorylation of STAT3 was inhibited by depletion of MET, HER2, or RET (Figure 4A). We further examined the effects of depletion of these RTKs on cell proliferation and apoptosis in *MET* amplification-positive cells. Depletion of MET resulted in marked inhibition of cell proliferation and induced a substantial level of apoptosis in these cells, whereas depletion of EGFR, HER2, or HER3 elicited similar effects but to a lesser extent (Figure 4B and C). Depletion of RET had little effect on cell proliferation or apoptosis. Finally, we examined the effects of RTK depletion on cell migration. Depletion of MET, HER2, or RET reduced the number of migrated cells compared with that apparent for cells transfected with a control siRNA, whereas depletion of EGFR or HER3 had no substantial effect on the migration of EBC-1 or H1993 cells (Figure 4D). Together, these results suggested that MET, EGFR, HER2, and HER3 activate AKT and ERK signalling pathways and promote cell proliferation and survival in lung cancer cells with *MET* amplification, whereas MET, HER2, and RET activate the STAT3 signalling pathway and promote cell migration.

DISCUSSION

We have here shown that MET associates with EGFR, HER2, HER3, and RET, and that these heterodimerisation partners of MET are highly phosphorylated in lung cancer cells positive for *MET* amplification. MET was previously shown to associate with HER3 in EGFR–TKI-resistant NSCLC cells with acquired *MET* amplification (Engelman *et al*, 2007), but the regulation of such association has remained unclear. We have now found that MET also forms a complex with HER3 in lung cancer cells with endogenous amplification of *MET* and that the heterodimer was dissociated as a result of inhibition of MET kinase activity. Given that HER3 is a kinase-inactive protein and requires a dimerisation partner to become phosphorylated (Guy *et al*, 1994; Kim *et al*, 1998; Holbro *et al*, 2003), our data indicate that the kinase activity of MET is

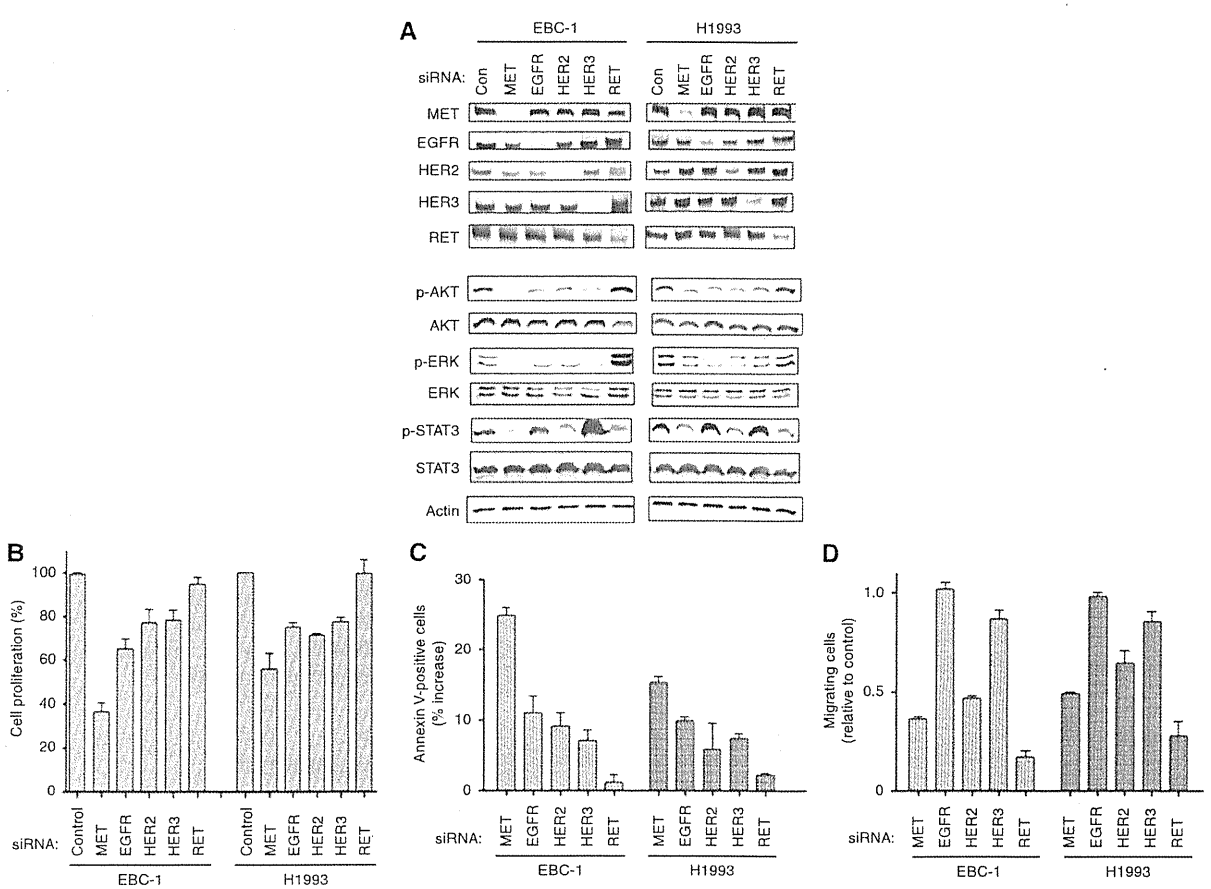

Figure 4 Effects of depletion of MET, EGFR, HER2, HER3, or RET on cell proliferation, apoptosis, and migration in lung cancer cells with *MET* amplification (**A**), EBC-1 and H1993 cells were transfected with MET, EGFR, HER2, HER3, RET, or nonspecific (Con) siRNAs for 72 h, after which cell lysates were prepared and subjected to immunoblot analysis with antibodies to the indicated proteins. (**B**) Cells transfected as in (**A**) were evaluated for cell proliferation. Absorbance values were expressed as a percentage of that for cells transfected with a control siRNA. (**C**) Cells transfected as in (**A**) were evaluated for the proportion of apoptotic cells. Data are expressed as the percentage increase in the number of annexin V-positive cells relative to the corresponding value for cells transfected with a control siRNA. (**D**) Cells were transfected with the indicated siRNAs for 24 h and then transferred in serum-free medium to cell culture inserts of a transwell apparatus for 24 h. The number of cells that migrated toward complete medium was counted with the use of a light microscope. Data are expressed relative to the value for cells transfected with a control siRNA. Data in (**B**–**D**) are means ± s.e. from three independent experiments.

© 2011 Cancer Research UK

required for formation of the MET–HER3 heterodimer, which results in the phosphorylation of HER3, in lung cancer cells with *MET* amplification, although it remains unclear whether HER3 phosphorylation is mediated by MET directly or by another kinase that is activated by MET.

Dimerisation of RTKs is a key event in signal transduction (Olayioye *et al*, 2000), but much remains unknown with regard to the heterodimerisation partners of RTKs expressed on the surface of cancer cells. To identify heterodimerisation partners of MET in lung cancer cells with *MET* amplification in a comprehensive manner, we made use of an RTK array. With this approach, we identified several highly phosphorylated RTKs, including EGFR, HER2, HER3, and RET. Moreover, immunoprecipitation analysis revealed that each of these RTKs formed a heterodimer with MET, demonstrating for the first time that EGFR, HER2, HER3, and RET are the main heterodimerisation partners of MET in *MET* amplification-positive lung cancer cells. In contrast to HER3, EGFR, HER2, and RET each possess intrinsic kinase activity (Takahashi *et al*, 1988; Schlessinger, 2002). We found that the EGFR–TKI gefitinib did not inhibit EGFR phosphorylation in lung cancer cells with *MET* amplification. In addition, phosphorylation of HER2 or RET was not inhibited by the corresponding specific TKIs lapatinib or vandetanib. These results thus suggest that the observed phosphorylation of EGFR, HER2, and RET is not attributable to autophosphorylation. Moreover, we found that the MET–TKI PHA-665752 induced the dissociation of heterodimers containing MET and either EGFR, HER2, HER3, or RET, and that this effect was accompanied by dephosphorylation of these RTKs. Taken together, these data thus suggest that the association between MET and these RTKs is dependent on MET kinase activity and results in their trans-phosphorylation by MET in lung cancer cells with *MET* amplification.

We found that siRNA-mediated depletion of EGFR, HER2, or HER3 resulted in inhibition of cell proliferation and induction of apoptosis accompanied by inhibition of AKT and ERK signalling pathways in lung cancer cells with *MET* amplification, although these effects were less pronounced that were those of MET depletion. Given that these RTKs associate predominantly with MET, our data suggest that heterodimers of MET with EGFR, HER2, or HER3 activate AKT and ERK signalling and thereby promote cell proliferation and survival (Figure 5). EGFR, HER2, and HER3 appear to activate signalling by forming a complex with MET in a manner dependent on MET kinase activity rather than on their own kinase activity in lung cancer cells with *MET* amplification. We also found that heterodimers of MET with either HER2 or RET activate STAT3 signalling and likely thereby promote cell migration (Figure 5). Heterodimerisation of MET with different partners thus appears to result in different downstream effects, although the underlying mechanisms responsible for such differences remain to be elucidated. Activation of the kinase JAK by growth hormone has been shown to result in phosphorylation of EGFR and consequent activation of the ERK signalling pathway. This activation of the ERK pathway is not dependent on the kinase activity of EGFR, but is mediated by docking sites on EGFR for Grb2, consistent with the notion that RTKs may also contribute to signal transduction by functioning as adaptor proteins (Yamauchi *et al*, 1997). It is thus possible that trans-phosphorylated EGFR, HER2, HER3, and RET act as scaffold proteins to promote downstream signalling of MET in lung cancer cells with *MET* amplification. Given that inhibition of MET kinase activity resulted in inhibition of signalling pathways activated by all the heterodimers of MET with the other RTKs, MET seems to be positioned at the apex of a signalling network in *MET* amplification-positive lung cancer cells, explaining why MET inhibition is associated with pronounced antitumour effects in these cells.

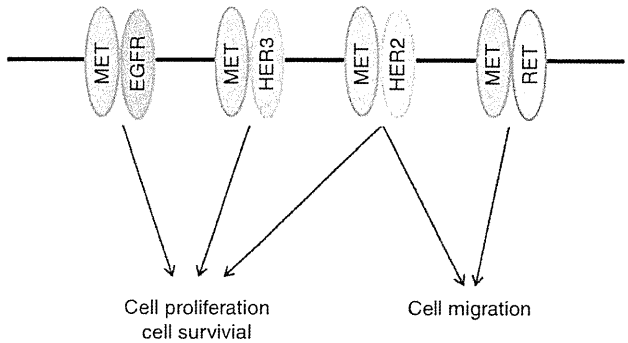

Figure 5 Proposed model for the roles of signalling pathways activated by heterodimers of MET and either EGFR, HER2, HER3, or RET in lung cancer cells with *MET* amplification.

We found that, whereas HER3 depletion resulted in downregulation of AKT and ERK phosphorylation, it appeared to induce upregulation of STAT3 phosphorylation in cells with *MET* amplification. Furthermore, depletion of RET inhibited STAT3 phosphorylation but appeared to increase ERK phosphorylation in such cells. Inhibition of one signalling pathway has previously been found to result in activation of other signalling pathways (Carracedo *et al*, 2008; Hoeflich *et al*, 2009; Pratilas *et al*, 2009). Such feedback regulation might explain the increases in STAT3 and ERK phosphorylation observed in this study, although further investigation is required to evaluate this notion.

In conclusion, our results suggest that EGFR, HER2, HER3, and RET are trans-phosphorylated by MET and promote cell proliferation and survival or cell migration as heterodimerisation partners of MET in lung cancer cells with *MET* amplification (Figure 5). Targeted therapeutic approaches for lung cancer, including treatment with TKIs for EGFR or the fusion protein EML4-ALK, have seen substantial progress over the last few years (Sequist *et al*, 2008; Kwak *et al*, 2010). Although amplification of *MET* is not common in NSCLC, lung tumours with *MET* amplification are highly dependent on MET signalling for their development (Lutterbach *et al*, 2007). Amplification of *MET* may thus define a subgroup of tumours that are susceptible to targeted kinase inhibition. An understanding of signal transduction in tumours with *MET* amplification will thus be important for further development of MET-targeted therapy. Our study provides new insight into the functional roles of trans-phosphorylated RTKs in *MET* amplification-positive lung cancer.

ACKNOWLEDGEMENTS

We thank E Hatashita, K Kuwata, and H Yamaguchi for technical assistance.

REFERENCES

Asahina H, Yamazaki K, Kinoshita I, Sukoh N, Harada M, Yokouchi H, Ishida T, Ogura S, Kojima T, Okamoto Y, Fujita Y, Dosaka-Akita H, Isobe H, Nishimura M (2006) A phase II trial of gefitinib as first-line therapy for advanced non-small cell lung cancer with epidermal growth factor receptor mutations. *Br J Cancer* **95**(8): 998–1004

Birchmeier C, Birchmeier W, Gherardi E, Vande Woude GF (2003) Met, metastasis, motility and more. *Nat Rev Mol Cell Biol* **4**(12): 915–925

© 2011 Cancer Research UK

Molecular Diagnostics

Carracedo A, Ma L, Teruya-Feldstein J, Rojo F, Salmena L, Alimonti A, Egia A, Sasaki AT, Thomas G, Kozma SC, Papa A, Nardella C, Cantley LC, Baselga J, Pandolfi PP (2008) Inhibition of mTORC1 leads to MAPK pathway activation through a PI3K-dependent feedback loop in human cancer. *J Clin Invest* **118**(9): 3065–3074

Engelman JA, Zejnullahu K, Mitsudomi T, Song Y, Hyland C, Park JO, Lindeman N, Gale CM, Zhao X, Christensen J, Kosaka T, Holmes AJ, Rogers AM, Cappuzzo F, Mok T, Lee C, Johnson BE, Cantley LC, Janne PA (2007) MET amplification leads to gefitinib resistance in lung cancer by activating ERBB3 signaling. *Science* **316**(5827): 1039–1043

Guy PM, Platko JV, Cantley LC, Cerione RA, Carraway III KL (1994) Insect cell-expressed p180erbB3 possesses an impaired tyrosine kinase activity. *Proc Natl Acad Sci USA* **91**(17): 8132–8136

Hoeflich KP, O'Brien C, Boyd Z, Cavet G, Guerrero S, Jung K, Januario T, Savage H, Punnoose E, Truong T, Zhou W, Berry L, Murray L, Amler L, Belvin M, Friedman LS, Lackner MR (2009) *In vivo* antitumor activity of MEK and phosphatidylinositol 3-kinase inhibitors in basal-like breast cancer models. *Clin Cancer Res* **15**(14): 4649–4664

Holbro T, Beerli RR, Maurer F, Koziczak M, Barbas III CF, Hynes NE (2003) The ErbB2/ErbB3 heterodimer functions as an oncogenic unit: ErbB2 requires ErbB3 to drive breast tumor cell proliferation. *Proc Natl Acad Sci USA* **100**(15): 8933–8938

Jo M, Stolz DB, Esplen JE, Dorko K, Michalopoulos GK, Strom SC (2000) Cross-talk between epidermal growth factor receptor and c-Met signal pathways in transformed cells. *J Biol Chem* **275**(12): 8806–8811

Kim HH, Vijapurkar U, Hellyer NJ, Bravo D, Koland JG (1998) Signal transduction by epidermal growth factor and heregulin via the kinase-deficient ErbB3 protein. *Biochem J* **334**(Pt 1): 189–195

Kwak EL, Bang YJ, Camidge DR, Shaw AT, Solomon B, Maki RG, Ou SH, Dezube BJ, Janne PA, Costa DB, Varella-Garcia M, Kim WH, Lynch TJ, Fidias P, Stubbs H, Engelman JA, Sequist LV, Tan W, Gandhi L, Mino-Kenudson M, Wei GC, Shreeve SM, Ratain MJ, Settleman J, Christensen JG, Haber DA, Wilner K, Salgia R, Shapiro GI, Clark JW, Iafrate AJ (2010) Anaplastic lymphoma kinase inhibition in non-small-cell lung cancer. *N Engl J Med* **363**(18): 1693–1703

Lai AZ, Abella JV, Park M (2009) Crosstalk in Met receptor oncogenesis. *Trends Cell Biol* **19**(10): 542–551

Lutterbach B, Zeng Q, Davis LJ, Hatch H, Hang G, Kohl NE, Gibbs JB, Pan BS (2007) Lung cancer cell lines harboring MET gene amplification are dependent on Met for growth and survival. *Cancer Res* **67**(5): 2081–2088

Masuya D, Huang C, Liu D, Nakashima T, Kameyama K, Haba R, Ueno M, Yokomise H (2004) The tumour-stromal interaction between intratumoral c-Met and stromal hepatocyte growth factor associated with tumour growth and prognosis in non-small-cell lung cancer patients. *Br J Cancer* **90**(8): 1555–1562

Mueller KL, Yang ZQ, Haddad R, Ethier SP, Boerner JL (2010) EGFR/Met association regulates EGFR TKI resistance in breast cancer. *J Mol Signal* **5**: 8

Nakamura Y, Niki T, Goto A, Morikawa T, Miyazawa K, Nakajima J, Fukayama M (2007) c-Met activation in lung adenocarcinoma tissues: an immunohistochemical analysis. *Cancer Sci* **98**(7): 1006–1013

Okamoto W, Okamoto I, Yoshida T, Okamoto K, Takezawa K, Hatashita E, Yamada Y, Kuwata K, Arao T, Yanagihara K, Fukuoka M, Nishio K, Nakagawa K (2010) Identification of c-Src as a potential therapeutic target for gastric cancer and of MET activation as a cause of resistance to c-Src inhibition. *Mol Cancer Ther* **9**(5): 1188–1197

Olayioye MA, Neve RM, Lane HA, Hynes NE (2000) The ErbB signaling network: receptor heterodimerization in development and cancer. *EMBO J* **19**(13): 3159–3167

Pratilas CA, Taylor BS, Ye Q, Viale A, Sander C, Solit DB, Rosen N (2009) (V600E)BRAF is associated with disabled feedback inhibition of RAF-MEK signaling and elevated transcriptional output of the pathway. *Proc Natl Acad Sci USA* **106**(11): 4519–4524

Schlessinger J (2002) Ligand-induced, receptor-mediated dimerization and activation of EGF receptor. *Cell* **110**(6): 669–672

Sequist LV, Martins RG, Spigel D, Grunberg SM, Spira A, Janne PA, Joshi VA, McCollum D, Evans TL, Muzikansky A, Kuhlmann GL, Han M, Goldberg JS, Settleman J, Iafrate AJ, Engelman JA, Haber DA, Johnson BE, Lynch TJ (2008) First-line gefitinib in patients with advanced non-small-cell lung cancer harboring somatic EGFR mutations. *J Clin Oncol* **26**(15): 2442–2449

Smolen GA, Sordella R, Muir B, Mohapatra G, Barmettler A, Archibald H, Kim WJ, Okimoto RA, Bell DW, Sgroi DC, Christensen JG, Settleman J, Haber DA (2006) Amplification of MET may identify a subset of cancers with extreme sensitivity to the selective tyrosine kinase inhibitor PHA-665752. *Proc Natl Acad Sci USA* **103**(7): 2316–2321

Takahashi M, Buma Y, Iwamoto T, Inaguma Y, Ikeda H, Hiai H (1988) Cloning and expression of the ret proto-oncogene encoding a tyrosine kinase with two potential transmembrane domains. *Oncogene* **3**(5): 571–578

Trusolino L, Comoglio PM (2002) Scatter-factor and semaphorin receptors: cell signalling for invasive growth. *Nat Rev Cancer* **2**(4): 289–300

Yamauchi T, Ueki K, Tobe K, Tamemoto H, Sekine N, Wada M, Honjo M, Takahashi M, Takahashi T, Hirai H, Tushima T, Akanuma Y, Fujita T, Komuro I, Yazaki Y, Kadowaki T (1997) Tyrosine phosphorylation of the EGF receptor by the kinase Jak2 is induced by growth hormone. *Nature* **390**(6655): 91–96

Zhao X, Weir BA, LaFramboise T, Lin M, Beroukhim R, Garraway L, Beheshti J, Lee JC, Naoki K, Richards WG, Sugarbaker D, Chen F, Rubin MA, Janne PA, Girard L, Minna J, Christiani D, Li C, Sellers WR, Meyerson M (2005) Homozygous deletions and chromosome amplifications in human lung carcinomas revealed by single nucleotide polymorphism array analysis. *Cancer Res* **65**(13): 5561–5570

This work is published under the standard license to publish agreement. After 12 months the work will become freely available and the license terms will switch to a Creative Commons Attribution-NonCommercial-Share Alike 3.0 Unported License.

Molecular Diagnostics

Jpn J Clin Oncol 2011;41(9)1132–1137
doi:10.1093/jjco/hyr102
Advance Access Publication 4 August 2011

LKB1 Mutations Frequently Detected in Mucinous Bronchioloalveolar Carcinoma

Atsushi Osoegawa, Takuro Kometani, Kaname Nosaki, Kaoru Ondo, Motoharu Hamatake, Fumihiko Hirai, Takashi Seto, Kenji Sugio* and Yukito Ichinose

Department of Thoracic Oncology, National Kyushu Cancer Center, Fukuoka, Japan

*For reprints and all correspondence: Kenji Sugio, Department of Thoracic Oncology, National Kyushu Cancer Center, Notame 3-1-1, Minami-ku, Fukuoka 811-1395, Japan. E-mail: sugio.k@nk-cc.go.jp

Received April 6, 2011; accepted June 18, 2011

Objective: *LKB1* mutations are common in patients with Peutz–Jeghers syndrome, which is characterized by mucocutaneous pigmentation, intestinal polyps and a high incidence of cancers at variable sites. This study investigated the status of the *LKB1* gene in mucinous bronchioloalveolar carcinoma with or without Peutz–Jeghers syndrome.
Methods: Three mucinous bronchioloalveolar carcinoma tumors from two Peutz–Jeghers syndrome patients and seven tumors from sporadic mucinous bronchioloalveolar carcinoma patients were collected by surgery between 2002 and 2008, and high molecular weight genomic DNA was extracted from them. The nucleotide sequences in exons 1–9 of *LKB1* were determined by genomic polymerase chain reaction-direct sequencing. The loss of heterozygosity was analyzed by high-resolution fluorescent microsatellite analysis using two microsatellite markers that encompass the *LKB1* locus, D19S886 and D19S565. The mutations of *KRAS*, *EGFR* and *p53* were also evaluated.
Results: The germline mutation of *LKB1* in the Peutz–Jeghers syndrome patients was identified as G215D by analyzing genomic DNA from normal lung tissue specimens. Furthermore, two of the three mucinous bronchioloalveolar carcinomas from these Peutz–Jeghers syndrome patients exhibited additional somatic mutations. On the other hand, four of seven sporadic 'non-Peutz–Jeghers syndrome' mucinous bronchioloalveolar carcinomas had *LKB1* mutations. Loss of heterozygosity analyses revealed allelic loss in two tumors with *LKB1* mutations. As a result, 70% of the mucinous bronchioloalveolar carcinomas exhibited *LKB1* mutations. *KRAS*, *EGFR* and *p53* mutations were mutually exclusive and observed in four, two and one tumors, respectively. Among them, five mutations occurred concomitantly with *LKB1* mutations.
Conclusions: The relatively high frequency of *LKB1* mutations in mucinous bronchioloalveolar carcinoma patients may therefore suggest its involvement in lung carcinogenesis, at least in mucinous bronchioloalveolar carcinoma.

Key words: tumor suppressor gene – hereditary disease – bronchioloalveolar carcinoma – loss of heterozygosity

INTRODUCTION

Liver kinase B1 (*LKB1*) is a gene encoding a serine–threonine kinase, which was initially deposited in the database by Nezu et al. in 1996, without writing a published report, in a screen aimed at identifying new kinases. In 1997, Hemminki et al. (1) revealed that the locus responsible for Peutz–Jeghers syndrome (PJS) was located on chromosome 19p13.3, where they then found the locus encoding *LKB1* with diverse mutations in PJS families (2). Another group also reported mutations in the *LKB1* gene

© The Author (2011). Published by Oxford University Press. All rights reserved.

Downloaded from http://jjco.oxfordjournals.org/ at National Cancer Centre (JMLA) on February 25, 2012

Table 1. *LKB1* mutations in mBACs

Tumor	Age	Sex	PYI	Size (mm)	LOH at D19S886	*LKB1* mutation									LOH at D19S565	*KRAS*	*EGFR*	*p53*
						EX01	02	03	04	05	06	07	08	09				
PJS																		
1	68	F	0	82	NI					E223L	G251D[a]				−	G12C		
2	43	F	0	29	NI	Y60X					G251D[a]				−	G12V		
3[b]	44	F	0	10	NI						G251D[a]				−			
Non-PJS																		
4	65	F	20	43	+								F354L		+		Del EX19	
5	69	M	42	90	NI				D194H						+			Y220C
6	55	F	44	59	−	D53T-63X									NI		Del EX19	
7	79	F	0	8	NI								F354L		NI			
8	61	M	82	10	−										−	G12D		
9	76	M	47	15	−										−	G12D		
10	69	M	66	29	NI										NI			

LKB1, liver kinase B1; mBACs, mucinous bronchioloalveolar carcinoma; PYI, pack-year index; LOH, loss of heterozygosity; PJS, Peutz–Jeghers syndrome; NI, not informative.
[a]Identical base substitution mutation confirmed in the germline.
[b]Tumor 3 is a secondary carcinoma that occurred in the PJS patients with tumor 2.

and called this enzyme serine–threonine kinase 11 (*STK11*) (3).

PJS is a rare autosomal-dominant disease characterized by mucocutaneous pigmentation and gastrointestinal hamartomatous polyposis (4,5). Furthermore, patients with PJS have an increased cancer risk, especially for cancers of gastrointestinal origin (6). Tumors arising from PJS are characterized by mucinous phenotypes, as are often observed in gastrointestinal tumors [i.e. adenoma malignum in the cervix (7), pancreatic adenocarcinoma (8) and intraductal pancreatic mucinous neoplasms (9)]. *LKB1* mutations are not as common in sporadic cancers except for non-small cell lung cancers (NSCLC) (10), about a third of which exhibit *LKB1* mutations (11–13). The representative mucinous NSCLC is mucinous bronchioloalveolar carcinoma (mBAC). mBAC is relatively rare among NSCLC, and there is only one case report of a PJS patient with mBAC (14).

The *LKB1* mutations in two PJS patients with mBAC were herein evaluated, along with sporadic cases of mBAC.

PATIENTS AND METHODS

Patients

Seventeen patients with mBAC were identified from 512 consecutive Japanese lung adenocarcinomas that underwent surgery at the Department of Thoracic Oncology, National Kyushu Cancer Center, from 2002 to 2008. Frozen tissue specimens were collected from 10 mBACs out of nine patients (four male and five female; age range: 43–79 years; median: 68 years; Table 1): 3 mBACs were derived from two PJS patients, who belonged to the same family. Tumor 1 was from a woman and Tumors 2 and 3 were from her daughter. Tumors 4–10 were from sporadic mBAC patients. Written informed consent was obtained from all patients, and ethical approval was obtained from the institutional review board of the National Kyushu Cancer Center. The histology of mBAC was determined based on hematoxylin and eosin staining according to the criteria of the World Health Organization (15). High-molecular-weight genomic DNA was extracted from the surgically resected specimens by standard phenol–chloroform methods and then was stocked in the bio-bank at our institute.

Mutation and Loss of Heterozygosity Analysis of the *LKB1* Gene

PCR primers were designed to cover all of the exons in the *LKB1* gene (Table 2). Twenty-five nanograms of genomic DNA from the bio-bank were used for each PCR amplification. The sequences of the primers are listed in Table 2. Direct sequencing of the PCR products was performed using the ABI Prism 310 Genetic Analyzer (Perkin-Elmer). All sequencing reactions were performed in both forward and reverse directions. Mutations were confirmed by an analysis of at least two independent PCR amplifications.

Loss of heterozygosity (LOH) was analyzed by a high-resolution fluorescent microsatellite analysis (HRFMA)

Downloaded from http://jjco.oxfordjournals.org/ at National Cancer Centre (JMLA) on February 25, 2012

using two microsatellite markers (D19S886 and D19S565) that encompass the *LKB1* locus. Specific primers were designed for these microsatellite markers (Table 2). Separation was done with a four-color laser-induced fluorescence capillary electrophoresis system (ABI Prism 310 Genetic Analyzer, Perkin-Elmer). The collected data were evaluated using the Genescan analysis software package 310 Genescan v. 3.1.2 (16).

Mutation Analysis of the *EGFR*, *KRAS* and *p53* Genes

Genomic PCR-direct sequencing was performed for exons 18–21 of the epidermal growth factor receptor (*EGFR*) gene, for codons 12–13 of the *KRAS* gene and for exons 5–9 of the *p53* gene (17,18). The detailed sequences of the primers are available on request.

Table 2. Primers used for analyses

LKB1	Primer sequences	
	Forward	Reverse
EX01	5′-aacacaaggaaggaccgctc-3′	5′-aagacagaaccatcagcacc-3′
EX02	5′-aggtacgccacttccacagg-3′	5′-ccattgccacaatggctgac-3′
EX03	5′-ccttttcagaggggtggctgag-3′	5′-tatcaggacaagcagtgtgg-3′
EX04	5′-cctggacttctgtgacttcc-3′	5′-cgaacgggtgcagtgcctgtg-3′
EX05	5′-caccctcaaaatctccgacc-3′	5′-agctgcccaagacgcagagg-3′
EX06	5′-cgtcaaccaccttgactgac-3′	5′-ccaaccctacatttctgcac-3′
EX07	5′-aggagcgtccaggtatcac-3′	5′-ctagcgcccgctcaaccag-3′
EX08	5′-ctgggtcggaaaactggacc-3′	5′-gacgtgggattggccaccag-3′
EX09	5′-ttcaggctggatacacctgg-3′	5′-ggtcaccatgactgactagc-3′
D19S565	5′-tcgaggcagcgtgattgcac-3′	5′-gatcattcctgtagtgatgc-3′
D19S886	5′-cattttactggctggcacttg-3′	5′-gtgttgggaacattcagctc-3′

RESULTS

LKB1 Mutations in PJS Patients

The *LKB1* mutation in PJS was confirmed by analyzing the genomic DNA from normal lung tissue specimens. Both patients, the mother and her daughter, were proven to possess the G251D mutation. The same mutation was observed in the three tumors derived from those patients. In addition, the mother's tumor had E223L, and one of the daughter's tumors had Y60X. Both of these two tumors are thought to have compound heterozygotes. LOH were not informative in these three tumors (Table 1).

LKB1 Mutations in Sporadic mBACs

Four of the seven sporadic mBACs had *LKB1* mutations: F354L in two and D194H and 63-stop in one each. LOH analyses revealed definite allelic loss in Tumor 4 (LOH was positive for both D19S886 and D19S565) and possible allelic loss in Tumor 5 (LOH was positive for D19S565 but not informative for D19S886). These results therefore explain one distinct (Tumor 4) and another possible (Tumor 5) biallelic inactivation of *LKB1* (Fig. 1). The other two sporadic cases exhibited neither LKB1 mutations nor LOHs.

Finally, 70% of mBACs exhibited LKB1 mutations. An analysis of the sporadic cases, excluding the PJS cases, revealed that the percentage was still as high as 57%.

Mutations in *KRAS*, *EGFR* and *p53*

A *KRAS* mutation was observed in four tumors: G12D in two and G12C and G12V in one each. The deletion in exon 19 (del E746-A750) of *EGFR* was observed in two tumors. The *p53* mutation (Y220C) was observed in one tumor. The mutations in *KRAS, EGFR* and *p53* were mutually exclusive (Table 1). Commonly, LKB1 mutations co-existed with

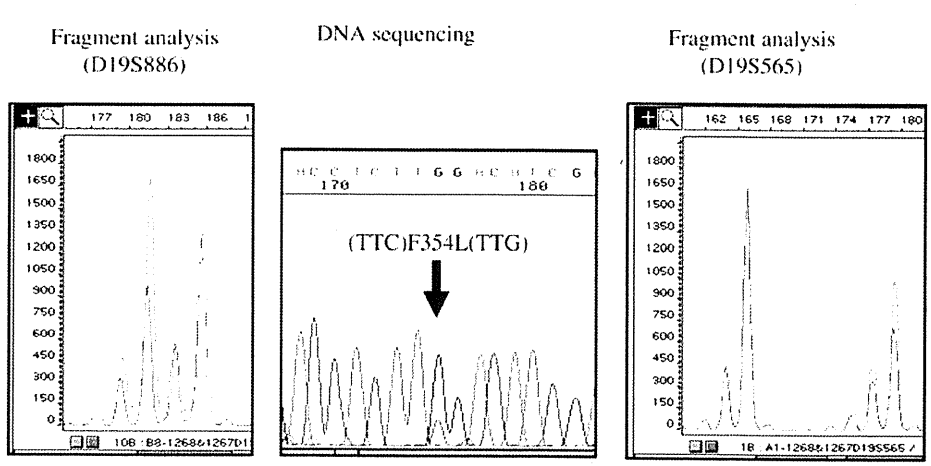

Figure 1. Representative mutation and loss of heterozygosity (LOH) analyses of *LKB1* are shown (Tumor 4). F354L was recognized at the black arrow by DNA sequencing. LOH was determined by fragment analyses using two microsatellite markers that encompassed the *LKB1* locus (D19S886 and D19S565).

Downloaded from http://jjco.oxfordjournals.org/ at National Cancer Centre (JMLA) on February 25, 2012

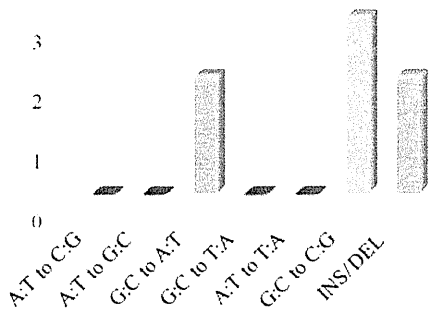

Figure 2. The spectrum of *LKB1* mutations is shown. G:C to A:T were E223L and G251D, and G:C to C:G were D194H and F354L. Y60X was a single-base insertion and D53T-63X was a single-base deletion.

KRAS mutations in Tumors 1 and 2, which are derived from familiar PJS cases; EGFR mutations in Tumors 4 and 6; and p53 mutation in Tumor 5.

Mutation Spectra of *LKB1* in mBAC

The mutation spectra of *LKB1* were analyzed. The germline mutation in the PJS pedigree was the G:C to A:T transition. The somatic mutations identified were one G:C to A:T transition, three G:C to C:G transversions, one single-nucleotide insertion and one single-nucleotide deletion (Fig. 2). None of the other mutations were observed.

The mutation spectra of *KRAS* and *p53* are G:C to T:A in two tumors, G:C to A:T in two tumors and T:A to C:G in one tumor. Both *EGFR* mutations were deletions.

DISCUSSION

The current study demonstrated the frequency of *LKB1* mutation in mBAC to be relatively high (4/7; 57%) in sporadic lung tumors; it was found in all of the tumors derived from PJS patients, although the frequency of *LKB1* mutation is reported to be 4–5% among lung cancers in Japan (19,20). *LKB1* mutations in lung cancer were related with male sex, smoking history and *KRAS* mutations (10,13,19,20). No significance of these parameters was observed in the current series, other than the relationship between *LKB1* mutation and mBAC. The mutations observed here have been reported in PJS patients, which inactivate kinase activity or impair farnesylation at the C-terminus (21,22).

Biallelic inactivation resulted from *LKB1* mutations with LOHs or from compound heterozygotes recognized in PJS cases account for the importance of *LKB1* mutation in mBAC tumorigenesis. *LKB1* is a tumor suppressor gene that causes G1 arrest when overexpressed (23). Further studies have shown that LKB1 acts as a master kinase controlling cellular polarity via MAP/microtubule affinity-regulating kinase, energy metabolism and the mammary target of the rapamycin (mTOR) pathway via AMP-activated protein kinase (AMPK) (24). Enterocytes with wild-type LKB1 differentiate and gain polarity once attached to the basal layer or become confluent; nevertheless, mutant LKB1 cannot gain polarity (25).

LKB1's role in polarity control was also confirmed from *in vivo* experiments by Shorning et al. (26). They also suggested the existence of possible relationships between LKB1 inactivation, polarity deregulation and excessive mucin production. They constructed a conditional knockout mouse model of LKB1. The epithelial cells of the mouse small intestine demonstrated an increased size and number of mucin-containing, goblet-cell-like cells when LKB1 was inactivated in the small intestines of mice by intraperitoneal injection of β-naphthoflavone. These undifferentiated cells showed features that were somewhere intermediate between Paneth and goblet cells (26). They concluded that these phenomena could explain the pathological aspect of polyp development in PJS patients, because alterations in goblet cells and elevated mucin production are commonly observed in hamartomas developing in PJS patients (27). Pathologically, similar features are observed in mBACs. mBAC cells are characterized by goblet cell dysplasia of the lining surface cells in the terminal respiratory unit, with excessive mucin production in the bronchioli and alveoli. 'Pure mucinous' colloid carcinomas, in which the immunohistochemical stains for luminal surface glycoproteins have shown inverted polarity, allow the colloid carcinoma cells to secrete mucin towards the stroma (28). It is therefore possible that such an LKB1 alteration would result in the deregulated polarity of mucin-producing cells, thereby leading to an overproduction of mucin, and an impaired differentiation of goblet cells, thus leading to uncontrolled proliferation. Further investigations are warranted to elucidate these hypotheses.

Homozygous *Lkb1*-deficient mice are lethal at midgestation by defects in the neural tube, mesenchymal cell death and vascular abnormalities (29). Heterozygous mice die of gastric polyps before forming carcinomas (30–32). However, heterozygous mice with other conditional mutants, such as *KRAS* (12), *p53* (33) or *PTEN* (34), show a malignant potential once one of those switches has either been turned on or off. Several oncogene mutations were identified among the mBACs with *LKB1* mutations. LKB1 loss could therefore be oncogenic even under heterozygous inactivation with other oncogenic mutations.

Several drugs have been tested against LKB1-causative tumors. Rapamycin, a macrolide antibiotic that inhibits the mTOR pathway, has been shown to reduce the gastric tumor burden in *Lkb1*(+/−) mice by oral administration (35). Metformin and phenformin, biguanides commonly used to treat diabetes, are some other candidates for treating those tumors. Biguanides inhibit ATP synthesis and thereby cause

Downloaded from http://jjco.oxfordjournals.org/ at National Cancer Centre (JMLA) on February 25, 2012

a rise in the cellular AMP:ATP ratio, which in turn activates AMPK (36). Several models have also indicated the possible therapeutic use of biguanides for tumors caused by LKB1-AMPK insufficiency (34,37).

In conclusion, frequent *LKB1* mutations were found in mBAC in both PJS cases and sporadic cases. LKB1 inactivation is therefore a possible cause of mBAC tumorigenesis. Furthermore, LKB1 may be a possible target of therapy for mBAC, using LKB1-targeted drugs, such as rapamycin and biguanides delivered either systemically or by airway inhalation.

Acknowledgements

We thank Yoko Takeda for her valuable technical assistance. We also thank Shinya Oda and Kenichi Taguchi, Department of Clinical Research, National Kyushu Cancer Center, for their critical comments and valuable technical advice.

Funding

This work was supported in part by a Grant-in-Aid for Cancer Research (16-1) from the Ministry of Health, Labour and Welfare of Japan and by a Grant-in-Aid for Young Scientists (B) No. 19790973 from the Japan Society for the Promotion of Science.

Conflict of interest statement

None declared.

References

1. Hemminki A, Tomlinson I, Markie D, Jarvinen H, Sistonen P, Bjorkqvist AM, et al. Localization of a susceptibility locus for Peutz–Jeghers syndrome to 19p using comparative genomic hybridization and targeted linkage analysis. *Nat Genet* 1997;15:87–90.
2. Hemminki A, Markie D, Tomlinson I, Avizienyte E, Roth S, Loukola A, et al. A serine/threonine kinase gene defective in Peutz–Jeghers syndrome. *Nature* 1998;391:184–7.
3. Jenne DE, Reimann H, Nezu J, Friedel W, Loff S, Jeschke R, et al. Peutz–Jeghers syndrome is caused by mutations in a novel serine threonine kinase. *Nat Genet* 1998;18:38–43.
4. Peutz J. On a very remarkable case of familial polyposis of the mucous membrane of the intestinal tract and nasopharynx accompanied by peculiar pigmentations of the skin and mucous membrane. *Ned Tijdschr Geneeskd* 1921;10:134–46.
5. Jeghers H, McKusick V, Katz K. Generalized intestinal polyposis and melanin spots of the oral mucosa, lips and digits; a syndrome of diagnostic significance. *N Engl J Med* 1949;241:1031–6.
6. Hearle N, Schumacher V, Menko FH, Olschwang S, Boardman LA, Gille JJ, et al. Frequency and spectrum of cancers in the Peutz–Jeghers syndrome. *Clin Cancer Res* 2006;12:3209–15.
7. Chen KT. Female genital tract tumors in Peutz–Jeghers syndrome. *Hum Pathol* 1986;17:858–61.
8. Luttges J, Stigge C, Pacena M, Kloppel G. Rare ductal adenocarcinoma of the pancreas in patients younger than age 40 years. *Cancer* 2004;100:173–82.
9. Sahin F, Maitra A, Argani P, Sato N, Maehara N, Montgomery E, et al. Loss of Stk11/Lkb1 expression in pancreatic and biliary neoplasms. *Mod Pathol* 2003;16:686–91.
10. Sanchez-Cespedes M. A role for LKB1 gene in human cancer beyond the Peutz–Jeghers syndrome. *Oncogene* 2007;26:7825–32.
11. Ding L, Getz G, Wheeler DA, Mardis ER, McLellan MD, Cibulskis K, et al. Somatic mutations affect key pathways in lung adenocarcinoma. *Nature* 2008;455:1069–75.
12. Ji H, Ramsey MR, Hayes DN, Fan C, McNamara K, Kozlowski P, et al. LKB1 modulates lung cancer differentiation and metastasis. *Nature* 2007;448:807–10.
13. Sanchez-Cespedes M, Parrella P, Esteller M, Nomoto S, Trink B, Engles JM, et al. Inactivation of LKB1/STK11 is a common event in adenocarcinomas of the lung. *Cancer Res* 2002;62:3659–62.
14. von Herbay A, Arens N, Friedl W, Vogt-Moykopf I, Kayser K, Muller KM, et al. Bronchioloalveolar carcinoma: a new cancer in Peutz–Jeghers syndrome. *Lung Cancer* 2005;47:283–8.
15. Travis W, Colby T, Corrin B, Shimosato Y, Brambilla E. *World Health Organization International Histological Classification of Tumors: Histological Typing of Lung and Pleural Tumors*. Vol. 1. Berlin Heidelberg, Germany: Springer-Verlag 1999;4.
16. Oda S, Oki E, Maehara Y, Sugimachi K. Precise assessment of microsatellite instability using high resolution fluorescent microsatellite analysis. *Nucleic Acids Res* 1997;25:3415–20.
17. Wataya H, Okamoto T, Maruyama R, Seto T, Yamazaki K, Tagawa T, et al. Prognostic factors in previously treated non-small cell lung cancer patients with and without a positive response to the subsequent treatment with gefitinib. *Lung Cancer* 2009;64:341–5.
18. Yamazaki K, Sugio K, Yamanaka T, Hirai F, Osoegawa A, Tagawa T, et al. Prognostic factors in non-small cell lung cancer patients with postoperative recurrence following third-generation chemotherapy. *Anticancer Res* 2010;30:1311–5.
19. Matsumoto S, Iwakawa R, Takahashi K, Kohno T, Nakanishi Y, Matsuno Y, et al. Prevalence and specificity of LKB1 genetic alterations in lung cancers. *Oncogene* 2007;26:5911–8.
20. Onozato R, Kosaka T, Achiwa H, Kuwano H, Takahashi T, Yatabe Y, et al. LKB1 gene mutations in Japanese lung cancer patients. *Cancer Sci* 2007;98:1747–51.
21. Boudeau J, Scott JW, Resta N, Deak M, Kieloch A, Komander D, et al. Analysis of the LKB1-STRAD-MO25 complex. *J Cell Sci* 2004;117:6365–75.
22. Yoo LI, Chung DC, Yuan J. LKB1—a master tumour suppressor of the small intestine and beyond. *Nat Rev Cancer* 2002;2:529–35.
23. Tiainen M, Ylikorkala A, Makela TP. Growth suppression by Lkb1 is mediated by a G(1) cell cycle arrest. *Proc Natl Acad Sci USA* 1999;96:9248–51.
24. Lizcano JM, Goransson O, Toth R, Deak M, Morrice NA, Boudeau J, et al. LKB1 is a master kinase that activates 13 kinases of the AMPK subfamily, including MARK/PAR-1. *EMBO J* 2004;23:833–43.
25. Baas AF, Kuipers J, van der Wel NN, Batlle E, Koerten HK, Peters PJ, et al. Complete polarization of single intestinal epithelial cells upon activation of LKB1 by STRAD. *Cell* 2004;116:457–66.
26. Shorning BY, Zabkiewicz J, McCarthy A, Pearson HB, Winton DJ, Sansom OJ, et al. Lkb1 deficiency alters goblet and paneth cell differentiation in the small intestine. *PLoS ONE* 2009;4:e4264.
27. Wang ZJ, Ellis I, Zauber P, Iwama T, Marchese C, Talbot I, et al. Allelic imbalance at the LKB1 (STK11) locus in tumours from patients with Peutz–Jeghers' syndrome provides evidence for a hamartoma-(adenoma)-carcinoma sequence. *J Pathol* 1999;188:9–13.
28. Adsay NV, Merati K, Nassar H, Shia J, Sarkar F, Pierson CR, et al. Pathogenesis of colloid (pure mucinous) carcinoma of exocrine organs: Coupling of gel-forming mucin (MUC2) production with altered cell polarity and abnormal cell-stroma interaction may be the key factor in the morphogenesis and indolent behavior of colloid carcinoma in the breast and pancreas. *Am J Surg Pathol* 2003;27:571–8.
29. Ylikorkala A, Rossi DJ, Korsisaari N, Luukko K, Alitalo K, Henkemeyer M, et al. Vascular abnormalities and deregulation of VEGF in Lkb1-deficient mice. *Science* 2001;293:1323–6.
30. Bardeesy N, Sinha M, Hezel AF, Signoretti S, Hathaway NA, Sharpless NE, et al. Loss of the Lkb1 tumour suppressor provokes intestinal polyposis but resistance to transformation. *Nature* 2002;419:162–7.

Downloaded from http://jjco.oxfordjournals.org/ at National Cancer Centre (JMLA) on February 25, 2012

31. Jishage K, Nezu J, Kawase Y, Iwata T, Watanabe M, Miyoshi A, et al. Role of Lkb1, the causative gene of Peutz–Jegher's syndrome, in embryogenesis and polyposis. *Proc Natl Acad Sci USA* 2002;99:8903–8.
32. Miyoshi H, Nakau M, Ishikawa TO, Seldin MF, Oshima M, Taketo MM. Gastrointestinal hamartomatous polyposis in Lkb1 heterozygous knockout mice. *Cancer Res* 2002;62:2261–6.
33. Nakau M, Miyoshi H, Seldin MF, Imamura M, Oshima M, Taketo MM. Hepatocellular carcinoma caused by loss of heterozygosity in Lkb1 gene knockout mice. *Cancer Res* 2002;62:4549–53.
34. Huang X, Wullschleger S, Shpiro N, McGuire VA, Sakamoto K, Woods YL, et al. Important role of the LKB1-AMPK pathway in suppressing tumorigenesis in PTEN-deficient mice. *Biochem J* 2008;412:211–21.
35. Robinson J, Lai C, Martin A, Nye E, Tomlinson I, Silver A. Oral rapamycin reduces tumour burden and vascularization in Lkb1(+/−) mice. *J Pathol* 2009;219:35–40.
36. El-Mir MY, Nogueira V, Fontaine E, Averet N, Rigoulet M, Leverve X. Dimethylbiguanide inhibits cell respiration via an indirect effect targeted on the respiratory chain complex I. *J Biol Chem* 2000;275:223–8.
37. Dowling RJ, Zakikhani M, Fantus IG, Pollak M, Sonenberg N. Metformin inhibits mammalian target of rapamycin-dependent translation initiation in breast cancer cells. *Cancer Res* 2007;67:10804–12.

Downloaded from http://jjco.oxfordjournals.org/ at National Cancer Centre (JMLA) on February 25, 2012

Lung Cancer 73 (2011) 375–378

Contents lists available at ScienceDirect

Lung Cancer

journal homepage: www.elsevier.com/locate/lungcan

Short communication

Signet ring cell adenocarcinoma of the lung with an *EML4–ALK* fusion gene mimicking mucinous (colloid) adenocarcinoma: A case report

Taro Ohba [a], Kenji Sugio [a,*], Takuro Kometani [a], Masafumi Yamaguchi [a], Motoharu Hamatake [a], Kaname Nosaki [a], Hiroaki Takeoka [a], Hiromoto Kitajima [a], Fumihiko Hirai [a], Takashi Seto [a], Kenichi Taguchi [b], Kenichi Nishiyama [b], Yoshitaka Shida [c], Yukito Ichinose [a]

[a] *Department of Thoracic Oncology, National Kyushu Cancer Center, 3-1-1 Notame, Minami-ku, Fukuoka 811-1395, Japan*
[b] *Cancer Pathology Laboratory, Institute for Clinical Research, National Kyushu Cancer Center, Fukuoka, Japan*
[c] *Department of Radiology, National Kyushu Cancer Center, Fukuoka, Japan*

ARTICLE INFO

Article history:
Received 18 January 2011
Received in revised form 2 April 2011
Accepted 20 May 2011

Key words:
Signet ring cell carcinoma
EML4–ALK
Non-small cell lung cancer
Surgery
Multiplex RT-PCR
Histopathology

ABSTRACT

We herein report a case of signet ring cell adenocarcinoma of the lung with an *EML4–ALK* fusion gene mimicking mucinous (colloid) adenocarcinoma. A 79-year-old female presented with a pulmonary tumor located in the right lower lobe measuring 21 mm in size. A right lower lobectomy was performed. The postoperative pathological examination revealed signet ring cell carcinoma with abundant mucin pools, and a multiplex RT-PCR analysis revealed the variant 2 inversion of the *EML4–ALK* gene.

© 2011 Elsevier Ireland Ltd. All rights reserved.

1. Introduction

Primary lung adenocarcinomas in which neoplastic cells float in large mucin pools are unusual, and their exact classification is still controversial. Signet ring cell carcinoma is an unusual subtype of adenocarcinoma of the lung. The most prominent pathological feature of this cancer is the intracellular mucin accumulation with a signet ring conformation [1]. Meanwhile, primary mucinous (colloid) adenocarcinoma (MC) is an extremely rare subtype of pulmonary adenocarcinoma that accounts for 0.24% of all lung cancers [2]. MC is described as a variant of adenocarcinoma by the latest edition of the world health organization (WHO) classification of lung cancers and was recently proposed to be colloid adenocarcinoma [1,3]. MC is pathologically characterized by a lesion with dissecting pools of mucin containing islands of neoplastic epithelium [1].

Recently, the echinoderm microtubule-associated protein-like 4 (*EML-4*)–anaplastic lymphoma kinase (*ALK*) gene inversion was detected in 6.7% of Japanese non-small cell lung cancer (NSCLC) patients [4]. The fusion gene encodes a constitutively active oncoprotein with an activated *ALK* kinase, resulting in the aberrant activation of downstream signaling targets including Akt, signal transducer and activator of transcription (STAT) 3, and Ras-extracellular signal regulated kinase (ERK) 1/2 [5]. Several series have reported the clinicopathological factors in patients with the *EML4–ALK* inversion [6,7]. *EML4–ALK* positive lung adenocarcinomas tended to be characterized by a less-differentiated grade, predominantly the acinar subtype or the signet-ring cell subtype in histology[6,7].

We herein report a case of primary signet ring cell adenocarcinoma mimicking MC with the inversion of the *EML4–ALK* gene.

2. Case report

A 79-year-old female who was a never smoker, was referred to our hospital because of left chest pain. Chest computed tomography (CT) performed as an initial screening showed an irregularly formed and well-defined nodule measuring 21 mm in the right lower lobe. The tumor was uniformly enhanced with regard to the density of the mediastinum (Fig. 1). Positron emission tomography (PET) with ^{18}F-fluorodeoxyglucose (FDG) showed positive activity in this lesion (maximum standardized uptake values (SUV_{max}); 4.78) and a hilar lymph node (SUV_{max}; 3.59). No metastatic tumor was detected by brain magnetic resonance imaging (MRI). The results of clinical examination and routine laboratory tests were within normal lim-

* Corresponding author. Tel.: +81 92 541 3231; fax: +81 92 551 4585.
E-mail address: sugio.k@nk-cc.go.jp (K. Sugio).

0169-5002/$ – see front matter © 2011 Elsevier Ireland Ltd. All rights reserved.
doi:10.1016/j.lungcan.2011.05.016

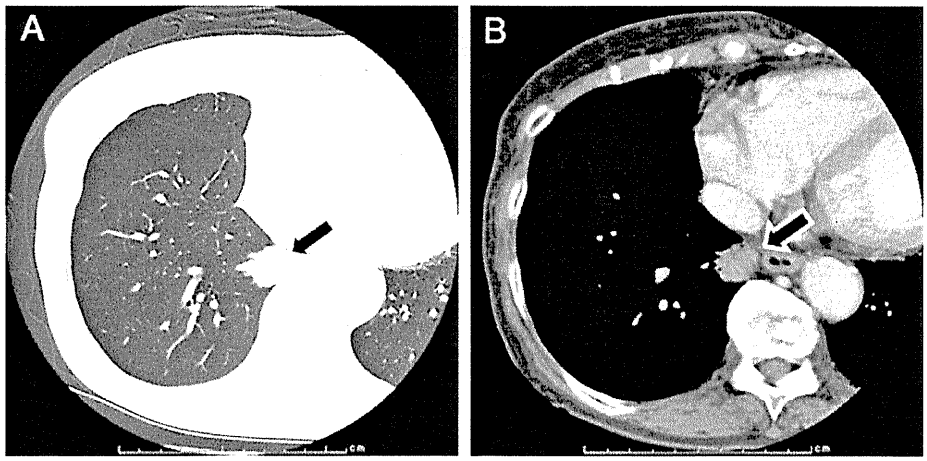

Fig. 1. CT demonstrated a round and well-defined nodule with spiculation measuring 21 mm in diameter in the right lower lobe (arrow). (A) The density of the lung. (B) The density of the mediastinum.

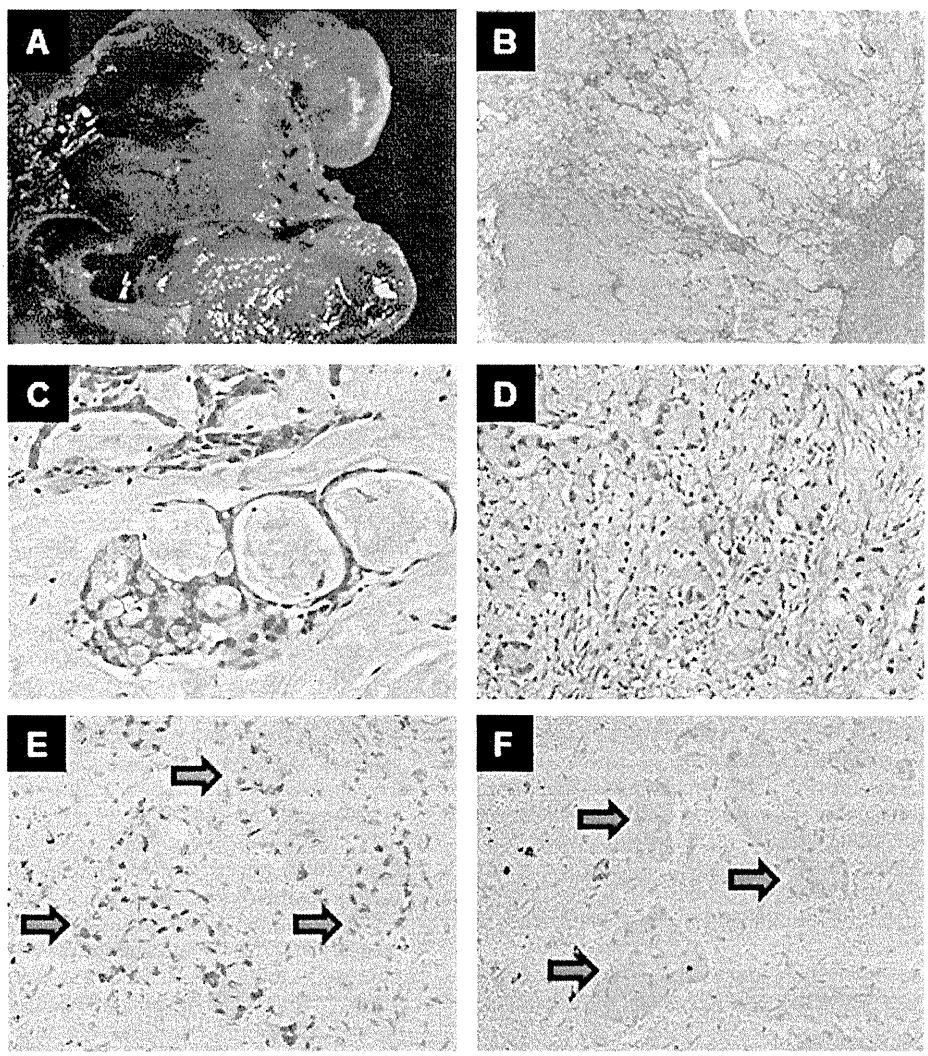

Fig. 2. (A) The cut surface of the tumor shows the nodule is well demarcated and filled with a yellowish-white gelatinous substance. (B) Two-thirds of the tumor was composed of abundant mucin pools that distended the alveoli. (H&E, objective lens magnification; 1.25×). (C and D) Foci of adenocarcinoma (H&E, objective lens magnification; 20×). (E) The nuclei and cytoplasm of the signet ring tumor cells in the fibrous stroma were positive for TTF-1 (arrows) (objective lens magnification; 20×). (F) The cytoplasm of the signet ring tumor cells was weakly positive for CEA (arrows) (objective lens magnification; 20×).